

SURFACE MODIFICATION OF POLYDIMETHYLSILOXANE WITH A
COVALENT ANTITHROMBIN-HEPARIN COMPLEX FOR BLOOD CONTACTING
APPLICATIONS

By

JENNIFER M. LEUNG, B.A.Sc.

A Thesis Submitted to the School of Graduate Studies in Partial Fulfillment
of the Requirements for the Degree Master of Applied Science

McMaster University

© Copyright by Jennifer M. Leung, April 2013

MASTER OF APPLIED SCIENCE (2013) McMaster University
(School of Biomedical Engineering) Hamilton, ON

TITLE: Surface Modification of Polydimethylsiloxane with a Covalent
Antithrombin-Heparin Complex for Blood Contacting
Applications

AUTHOR: Jennifer M. Leung,
B.A.Sc. (University of Toronto)

SUPERVISORS: Professor John L. Brash
Professor Anthony K.C. Chan

NUMBER OF PAGES: xiv, 81

ABSTRACT

Medical devices used for diagnosis and treatment often involve the exposure of the patient's blood to biomaterials that are foreign to the body, and blood-material contact may trigger coagulation and lead to thrombotic complications. Therefore, the risk of thrombosis and the issue of blood compatibility are limitations in the development of biomaterials for blood-contacting applications. The objective of this research was to develop a dual strategy for surface modification of polydimethylsiloxane (PDMS) to prevent thrombosis by (1) grafting polyethylene glycol (PEG) to inhibit non-specific protein adsorption, and (2) covalently attaching an antithrombin-heparin (ATH) covalent complex to the distal end of the PEG chains to inhibit coagulation at the surface.

Surface characterization via contact angle measurements confirmed reductions in hydrophobicity for the modified surfaces and x-ray photoelectron spectroscopy (XPS) indicated that heparin and ATH were present. The predisposition of PDMS to induce blood coagulation was investigated, and advantages of ATH over heparin in inhibiting coagulation on PDMS were demonstrated. Studies of protein interactions using radiolabelling and Western blotting demonstrated the ability of PEG-modified surfaces to resist non-specific protein adsorption, and the ability of ATH- and heparin-modified surfaces to specifically bind AT present in plasma, thereby providing anticoagulant activity. Through specific interactions with the pentasaccharide sequence on the heparin moiety, the ATH-modified surfaces bound AT more efficiently than the heparin-modified surfaces. Thromboelastography (TEG) was used to evaluate further the anticoagulant potential of the ATH-modified surfaces. It was found that coagulation occurred at a

slower rate on the ATH-modified surfaces compared to unmodified PDMS, and the resulting clot was mechanically weaker. By creating a surface with bioinert and bioactive properties, non-specific protein adsorption was reduced and anticoagulation at the surface through specific protein binding was promoted. This dual PEO/ATH modification strategy may therefore offer an improved approach for the minimization of thrombosis on PDMS and biomaterial surfaces more generally.

ACKNOWLEDGEMENTS

I would like to thank many people for their support and guidance during my time at McMaster, I would not be able to complete my project and degree without them. First I would like to thank my supervisors, Dr. John L. Brash and Dr. Anthony K.C. Chan. I am grateful for the opportunity to be a part of their research, and to work with academics with distinguished expertise in biomaterials and medicine. Dr. Brash, thank you for being such as supportive supervisor and mentor, your guidance in my research and feedback on my writing are invaluable to my professional development, and your dedication to good research will always be an example to me. Dr. Chan, I greatly appreciate your practical suggestions and advice from the medical perspective, and thank you for sharing your insights of studying medicine and working as a doctor with me.

Thank you to Dr. Christoph Fusch, Dr. Niels Rochow and Dr. Ravi Selvaganapathy for the opportunity to participate in the research and development of the oxygenator, as well as your support and suggestions in the oxygenator project.

I would like to thank Rena Cornelius, for always being available to help in the lab, and for all your valuable advice and suggestions on my research. I always look forward to seeing you in the lab, as there is something to learn in every conversation. I would also like to thank Les Berry, for your encouragement and advice, the enthusiasm that you show for your work is inspiring. I really appreciate all your prompt replies, in-depth explanations, and helpful suggestions on my project.

To members of the Brash group, Kyla, Sara and Yvanne, thank you for your friendship and support throughout my graduate experience, especially to Kyla for your

willingness to help and your advice on my project, and also to Yvanne for your helpfulness and hospitality during our trip to China.

To members of the Chan group, Helen Atkinson, Ivan Stevic, Ankush Chander, it was a pleasure to work with you, and special thanks to Jorell Gantioqui for helping me run the TEG experiments. I would also like to thank Wen Wu from the Selvaganapathy group, for all his help and practical suggestions on whatever I want to try with PDMS.

Lastly, I would like to thank my family. Mom and Dad, thank you for your love and continual support, always providing me with the best of everything. Aunt Helen, thank you for your invaluable advice to me as a researcher, especially for your help with my writing. To my brother, Colin, thank you for your care and understanding. I am truly grateful for my family and friends, and for all your support and encouragement.

ABSTRACT	III
ACKNOWLEDGEMENTS	V
LIST OF FIGURES	IX
LIST OF TABLES	XII
LIST OF ABBREVIATIONS	XIII
1. INTRODUCTION AND OBJECTIVES	1
2. LITERATURE REVIEW	3
2.1 BIOMATERIALS AND THROMBOSIS	3
2.2 BLOOD-MATERIAL INTERACTIONS.....	4
2.2.1 <i>Protein Adsorption</i>	5
2.2.2 <i>Coagulation</i>	7
2.3 INHIBITION OF COAGULATION	10
2.3.1 <i>Heparin</i>	10
2.3.2 <i>Antithrombin-Heparin (ATH) Covalent Complex</i>	15
2.4 SILICONES	19
2.4.1 <i>Silicone Structure</i>	19
2.4.2 <i>Silicone in Biomedical Applications</i>	19
2.4.3 <i>Surface Modification of Silicone</i>	20
2.5 THROMBOELASTOGRAPHY (TEG)	22
2.5.1 <i>Principle of Thromboelastography</i>	23
2.5.2 <i>Application of TEG in the Evaluation of Biomaterials</i>	24
3. MATERIALS AND METHODS	27
3.1 MATERIALS	27
3.2 METHODS.....	28
3.2.1 <i>Surface Preparation</i>	28
3.2.2 <i>Water Contact Angles</i>	30
3.2.3 <i>X-ray Photoelectron Spectroscopy (XPS)</i>	30
3.2.4 <i>Protein Radiolabelling</i>	30
3.2.5 <i>Protein Adsorption Experiments</i>	31
3.2.6 <i>Sodium Dodecyl Sulfate–Polyacrylamide Gel Electrophoresis (SDS–PAGE)</i> <i>and Western Blotting</i>	32
3.2.7 <i>Destruction of the Pentasaccharide Sequence in Heparin</i>	32
3.2.8 <i>Thromboelastography (TEG)</i>	33
3.3 STATISTICAL ANALYSIS	35

4. RESULTS	36
4.1 SURFACE CHARACTERIZATION.....	36
4.1.1 <i>Water Contact Angles</i>	36
4.1.2 <i>X-Ray Photoelectron Spectroscopy (XPS)</i>	38
4.2 PROTEIN INTERACTIONS.....	39
4.2.1 <i>ATH Surface Density and Stability</i>	39
4.2.2 <i>Fibrinogen Adsorption from Buffer</i>	41
4.2.3 <i>AT Adsorption from Plasma</i>	42
4.2.5 <i>Adsorption of antithrombin from plasma to NaIO₄-NaBH₄-treated surfaces</i> ...	46
4.2.6 <i>Western Blotting</i>	48
4.3 THROMBOELASTOGRAPHY (TEG).....	49
4.3.1 <i>TEG for PDMS modified with ATH by physical adsorption</i>	49
4.3.2 <i>TEG experiments on PDMS modified with covalently bound ATH via PEG spacer</i>	52
5. DEVELOPMENT OF BLOOD OXYGENATOR FOR NEONATES.....	56
5.1 INTRODUCTION.....	56
5.2 MATERIALS AND METHODS	59
5.2.1 <i>HSA adsorption on oxygenators: visualization with gold stain</i>	59
5.2.2 <i>HSA adsorption on oxygenators followed by incubation in buffer and determination of protein concentration</i>	60
5.2.3 <i>ATH adsorption on PDMS discs followed by incubation in blood</i>	61
5.3 RESULTS AND DISCUSSION.....	61
5.3.1 <i>HSA adsorption on oxygenators: visualization with gold stain</i>	61
5.3.2 <i>HSA adsorption to oxygenators followed by incubation in buffer and determination of residual protein by concentration measurements</i>	64
5.3.3 <i>ATH adsorption on PDMS discs followed by incubation in blood</i>	65
5.3.4 <i>Discussion and Conclusions</i>	66
6. SUMMARY AND RECOMMENDATIONS FOR FURTHER WORK.....	68
6.1 SUMMARY	68
6.2 RECOMMENDATIONS FOR FUTURE WORK	70
6.2.1 <i>Surface Modification with PEG and ATH</i>	70
6.2.2 <i>Interactions with other proteins and blood components</i>	72
6.2.3 <i>Thromboelastography (TEG)</i>	73
REFERENCES.....	74

LIST OF FIGURES

Figure 1. Coagulation cascade showing the intrinsic, extrinsic pathways and fibrinolysis (from: http://www.enzymeresearch.com/CASCADES_2004/images/CASCADE_eri_2007.pdf).

Figure 2. Schematic illustrating the inhibition of factor Xa and thrombin by antithrombin (AT) catalyzed by unfractionated heparin (UFH) (With permission from [34]).

Figure 3. Structure of the pentasaccharide sequence in heparin (adapted from [36]).

Figure 4. Schematic showing the synthesis of the ATH covalent complex from standard heparin, rectangular blocks on the heparin chains represent the pentasaccharide sequence, curve at end of heparin chain to blue AT molecule represents the covalent keto-amine linkage between aldose aldehyde and N-terminal amine (Courtesy of L. Berry, McMaster University).

Figure 5. Synthesis of the covalent ATH complex via Schiff base formation (a to b) and Amadori rearrangement (b to c) (adapted from [47]).

Figure 6. Trimethylsiloxy terminated polydimethylsiloxane (PDMS).

Figure 7. Functionalization of PDMS with SiH groups (adapted from [24]).

Figure 8. Hydrosilylation reaction involving a Si-H group and a terminal double bond catalyzed by a platinum catalyst [56].

Figure 9. (a) The TEG 5000 Thrombelastograph Hemostasis Analyzer System (Haemoscope Corporation, Niles, IL) (b) TEG cup and pin assembly that sits in the (white) holder during analysis (adapted from [66]).

Figure 10. Reference diagram for TEG curves. Parameters in figure are explained in Table 1. The x-axis is time (min); the y-axis is distance in mm reflecting clot strength (adapted from [62]).

Figure 11. Reaction scheme for grafting PEG on PDMS.

Figure 12. Reaction scheme for immobilizing ATH on PDMS previously functionalized with PEG.

Figure 13. Destruction of the Pentasaccharide Sequence in Heparin by chemical treatment with NaIO_4 and NaBH_4 (Courtesy of L. Berry, McMaster University).

Figure 14. Water contact angles of control PDMS and PDMS modified with PEG350 and PEG550. Advancing and receding angles measured by the sessile drop method. Data are mean \pm SD, $n \geq 12$.

Figure 15. ATH uptake from buffer on surfaces before and after SDS treatment. Surfaces were incubated in ATH (0.1 mg/mL in PBS, 5% radiolabelled) for 3 h. Data are mean \pm SD, $n = 3$.

Figure 16. Fibrinogen adsorption to PDMS surfaces modified with PEG and PEG-ATH. Fibrinogen concentration 1 mg/mL in PBS, 2% radiolabelled. Adsorption time 3 h. Adsorbed quantities determined from radioactivity before and after incubation in SDS overnight. Data are mean \pm SD, $n = 3$.

Figure 17. AT adsorption from plasma to PDMS surfaces modified with PEG, PEG-heparin and PEG-ATH. Adsorption time 3 h. Data are mean \pm SD, $n = 3$. * Significant differences ($p < 0.05$).

Figure 18. Antithrombin and fibrinogen adsorption from plasma to unmodified PDMS, and PDMS modified with PEG, PEG-heparin and PEG-ATH. Adsorption time 3 h. Data are mean \pm SD, $n = 4$. * Significant difference between surfaces in Fg adsorption ($p < 0.05$), ** significant difference between surfaces in AT adsorption ($p < 0.05$), *** significant difference between Fg and AT adsorption on the same surface ($p < 0.05$).

Figure 19. Antithrombin adsorption from plasma to PDMS surfaces modified with PEG and either ATH or heparin. Surfaces were treated or not treated with NaIO₄ and NaBH₄ to selectively destroy the AT-binding pentasaccharide sequence. Data are mean \pm SD, $n = 3$.

Figure 20. Western blots of proteins eluted from PDMS, PEG350, PEG350-ATH and PEG350-heparin surfaces after incubation in plasma. Blots were probed with antibodies against HMWK, fibrinogen (Fg), plasminogen, antithrombin (AT), C3, transferrin, fibronectin, albumin, immunoglobulin G (IgG), vitronectin (Vn) and apolipoprotein-AI (ApoAI).

Figure 21. TEG data shown in graphical form. Three separate runs are shown with: (a) PDMS, (b) PEG350-ATH, (c) PEG350-ATH. A single PDMS and two PEG350-ATH surfaces were tested. X-axis is time (min), y-axis is distance. The reaction time (R) was estimated from each graph.

Figure 22. Circulation of blood from the infant to the oxygenator via the umbilical vessels (from <http://bmc.erin.utoronto.ca/~erinw/d3.html>).

Figure 23. Different views of the oxygenator: (a) Schematic showing 14 modules stacked up in the oxygenator, direction of blood flow also indicated by arrows (b) View of (a)

without the skeleton structure, the 14 modules are connected in parallel (c) photograph of oxygenator with blood flow (d) single oxygenator module. (Adapted from [81]).

Figure 24. Single oxygenator module: (a) photograph, top view of module, (b) schematic of microfluidic network, (c) side view (Adapted from [80]).

Figure 25. Schematics (a&b) of oxygenator divided into sections for analysis.

Figure 26. Grid of micro-channels in oxygenator module after HSA adsorption and gold staining. Purple colour indicates protein adsorbed on the inside surface of the microchannels.

Figure 27. Microchannel grid showing regions blocked by air bubbles when PBS was circulated.

Figure 28. Desorption of ATH from PDMS discs in contact with blood. Data are mean \pm SD, n = 3.

LIST OF TABLES

Table 1. Explanation of parameters in TEG curves [62].

Table 2. Low resolution XPS data (atom %) for PDMS surfaces at 90° take-off angle (data precision, $\pm 5\%$).

Table 3. TEG results for unmodified PDMS and PDMS with ATH physically adsorbed. Data are means \pm SD (n = 2). Parameters: R (reaction time), K (coagulation time), α (rate of clot development), MA (maximum amplitude).

Table 4. HSA adsorption on grid before and after incubation with PBS.

Table 5. HSA adsorption on sections of grid before and after incubation with PBS (see Fig. 25b for nomenclature of grid sections).

LIST OF ABBREVIATIONS

AT	Antithrombin
ATH	Antithrombin-heparin complex
ApoAI	Apolipoprotein-AI
EC	Endothelial cell
F	Factor
Fg	Fibrinogen
HIT	Heparin-induced thrombocytopenia
HMWK	High molecular weight kininogen
HSA	Human serum albumin
IgG	Immunoglobulin
NHS	N-hydroxysuccinimide
PBS	Phosphate buffered saline
PDMS	Polydimethylsiloxane
PEG	Polyethylene glycol
PHMS	Polyhydromethylsiloxane
PTFE	Polytetrafluoroethylene
PVDF	Polyvinylidene fluoride
SDS	Sodium dodecyl sulfate
SDS-PAGE	Sodium dodecyl sulfate–polyacrylamide gel electrophoresis
SEM	Scanning electron microscopy
TAT	Thrombin-antithrombin complex

TEG	Thromboelastography
t-PA	Tissue plasminogen activator
UFH	Unfractionated heparin
Vn	Vitronectin
XPS	X-ray photoelectron spectroscopy

1. INTRODUCTION AND OBJECTIVES

A major limitation in the development of biomaterials for medical applications is the occurrence of coagulation and thrombosis when they contact blood [1]. A thrombotic event in a patient may lead to the development of pulmonary emboli, myocardial infarction, stroke, and organ failure. The formation of blood clots around an implant or a medical device may cause device failure [2]. These complications require additional medical intervention such as image-guided diagnosis, implant or medical device removal and replacement, medical or surgical treatment to remove the clots, and a further period of prophylactic anticoagulation for the patient, with its risks and expense. As a result, it is essential that blood-contacting biomaterials for clinical use be designed to incorporate an anticoagulant mechanism [1]. Polydimethylsiloxane (PDMS) is commonly used for biomedical devices such as catheters, oxygenators, and prosthetic heart valves [3–7]. However, PDMS adsorbs proteins strongly and extensively, and proteins adsorbed to surfaces in contact with blood may trigger adverse responses, including platelet adhesion, activation and aggregation [1,2,4,5]. Activated platelets provide a catalytic surface for coagulation reactions and platelet aggregates are an essential component of thrombi [10]. Therefore, surface modification is critical for overcoming these limitations [7–9].

Modification of biomaterial surfaces with heparin has been a popular approach to prevent blood coagulation [11]. A specific pentasaccharide sequence on the heparin molecule has high affinity for the thrombin inhibitor antithrombin (AT). This interaction induces a conformational change in antithrombin which increases its rate of reaction with thrombin by ~1000-fold [12]. Immobilization of heparin on biomaterials has been shown

to be effective in reducing surface thrombogenicity, but is limited by the relatively low activity of standard heparin preparations in which only about one-third of the heparin molecules contain the pentasaccharide AT-binding sequence [4,13]. Moreover, the immobilization process itself may interfere with the structure and orientation of the saccharide sequences, limiting their functional activity [11]. A novel anticoagulant, the antithrombin-heparin (ATH) covalent complex, has been developed to overcome the limitations of heparin [14]. The objective of this research was to develop PDMS surface-modified with polyethylene glycol and the ATH complex. The overall strategy was to control protein-surface interactions for the prevention of coagulation and thrombosis. Polyethylene glycol (PEG) was grafted on PDMS as a means of inhibiting non-specific protein adsorption, and the antithrombin-heparin (ATH) covalent complex was attached covalently to the distal chain end of the PEG to promote anticoagulation at the surface.

The research in this thesis provides new information on the surface modification of PDMS to improve blood compatibility. This includes information on plasma protein interactions with the modified surfaces, and on the coagulation response of the materials as assessed by thromboelastography (TEG) as well as more conventional methods. In addition, the PEG/ATH approach to modification of PDMS was applied to the development of a microfluidic PDMS blood oxygenator designed to provide respiratory support to premature infants.

2. LITERATURE REVIEW

2.1 Biomaterials and Thrombosis

Biomaterials are used in medical devices such as heart valve prostheses and artificial hip joints that replace the function of injured or diseased tissues [15]. Biomaterials are also used in the construction of medical devices designed to replace a specific function of the body, such as the artificial kidney and the intraocular lens. Generally speaking, biomaterials are functional materials that are intended to interact with a biological system in a specific manner and therefore must therefore have “the ability to perform with an appropriate host response in a specific application, without causing adverse effects to the surrounding environment”, which is the essence of biocompatibility according to Williams [16].

The biocompatibility of a material is related to its function, application and local environment [16]. Therefore, blood compatibility is an important aspect to consider in the design and selection of biomaterials for blood-contacting applications. Blood-material contact can trigger adverse events including thrombosis, thromboembolism, immunological reactions, toxic effects, and haemolytic damage [1,10]. For example, membrane oxygenators are used in cardiac surgery that requires cardiopulmonary bypass. The patient’s blood is pumped across a series of membranes that allow gas exchange to take place, but contact of the blood with the membranes, tubing and pump of the oxygenator system over several hours can result in hemolytic damage and thrombus formation on the oxygenator surfaces [17]. To prevent coagulation, large doses of heparin (300 units/kg) are usually administered and prostacyclin can also be administered as an

antiplatelet agent [17,18]. However, such systemic anticoagulation may lead to haemorrhagic complications and increase the need for transfusion, thus increasing the risks of the surgery and extending the time required for recovery [18].

The occurrence of thrombosis is a major limitation in the development of blood-contacting devices, since thrombus accumulation can compromise device function and efficacy, leading to device failure [17]. For example, catheters for arterial and venous access are generally used for the intravenous administration of fluids. Thrombus formation may occur within the catheter, on the exterior of the catheter (forming a “sleeve”), and on the vessel wall where the catheter is in contact [17]. Although no synthetic material is as thromboresistant as the natural vascular endothelium, biomaterial design aims to reduce thrombogenicity in order to improve biocompatibility.

Much research has been done on blood-material interactions since the 1980s largely with a view to improving understanding of the influence of artificial materials on coagulation. By gaining a better understanding of how blood-material contact leads to thrombosis, surface properties that contribute to blood compatibility and reduced thrombogenicity can be identified to aid in improving the design and selection of biomaterials for various blood-contacting applications [19].

2.2 Blood-Material Interactions

Blood-material contact triggers protein adsorption, platelet adhesion and aggregation, initiation of coagulation, complement activation, and adhesion of erythrocytes and leukocytes [10,19]. It is generally accepted that protein adsorption

occurs within seconds of contact, triggers and mediates the above responses which occur simultaneously and are often interdependent [1,10].

2.2.1 Protein Adsorption

Protein adsorption is understood as a critical and important process in blood-material interactions because it occurs rapidly after blood-material contact, resulting in a layer of adsorbed protein that determines subsequent blood-material interactions [17]. For example, the adsorption of factor XII activates the intrinsic pathway of coagulation, and adsorbed fibrinogen promotes the adhesion of platelets [20]. Adsorbed fibrinogen may be exchanged with high molecular weight kininogen (HMWK), a protein participating in the activation of intrinsic coagulation [19]. Adams and Feuerstein showed that quantities of adsorbed fibrinogen as low as 5 ng/cm^2 can increase platelet adhesion by 20-fold [21].

2.2.1.1 Surface Modification to Control Protein Adsorption

Protein adsorption occurs mainly by non-covalent interactions, including hydrogen bonding, electrostatic interactions and hydrophobic interactions [22]. Generally speaking, it can be understood that almost all proteins adsorb to all surfaces, but specific surface and protein properties affect the rate, extent, and mechanism of adsorption, as well as the conformation of the adsorbed proteins and the composition of the layer in multiprotein systems. These factors all contribute to blood-material interactions subsequent to protein adsorption, and ultimately affect the thrombogenicity of the surface [1,22]. The strategy of improving blood compatibility pursued in the present work focuses

on modifying the properties of the surface to control protein-surface interactions, including minimizing nonspecific adsorption (bio-inert approach) and promoting specific adsorption (bio-active approach) [1].

The goal of the bioinert approach is to develop an inert or non-fouling surface that resists protein adsorption in order to prevent subsequent responses such as platelet adhesion and activation of coagulation factors. For example, albumin has been used to passivate the surface of biomaterials [23], and polyethylene glycol (PEG) has been widely applied to provide resistance to non-specific adsorption, as well as to cell and bacterial adhesion [24]. PEG is a water soluble, non-toxic polymer, with structure $(-\text{CH}_2\text{CH}_2\text{O}-)_n$ [24]. Mechanisms proposed to explain the protein resistance of PEG include steric repulsion, osmotic repulsion and water interactions [15]. Steric repulsion represents physical resistance. Since the PEG chain is highly flexible, it is easily compressed when approached by a protein; it then repels the protein in order to retain its unperturbed conformation [15]. In osmotic repulsion the effective concentration of polymer segments in the layer increases as the protein approaches, thus increasing the osmotic pressure and generating a repulsive force. PEG is water soluble and strongly hydrophilic; it forms hydrogen bonds with water molecules to create a “water cage” around the PEG chains on the surface, thus creating a water barrier and limiting protein access to the surface [15]. Factors such as the chain length, surface coverage and grafting density of PEG chains also influence its protein resistance [15,25].

The bioactive approach aims to achieve an appropriate bioactivity by promoting the adsorption of specific proteins. Examples in the blood compatibility field include

surface attachment of heparin to promote adsorption of antithrombin, hirudin to promote thrombin adsorption/neutralization, and lysine to promote plasminogen and tissue plasminogen activator (t-PA) adsorption for clot lysis [26,27].

2.2.2 Coagulation

In the body coagulation generally occurs in response to blood vessel damage in order to arrest bleeding, and includes interactions among clotting factors, platelets and endothelial cells [28]. Coagulation can also be triggered by contact activation when blood comes in contact with a foreign material, i.e. a material other than the endothelium.

The coagulation cascade shown in Fig. 1 describes the sequence of reactions that occurs in the blood from initiation to the formation of fibrin, the material of the clot. The clotting factors are normally inactive, but become enzymatically active through proteolytic cleavage by activated clotting factors higher in the cascade to drive the coagulation response [10]. In the classical understanding of the coagulation process, the intrinsic and extrinsic systems converge to a common pathway that leads to the production of thrombin, and thrombin catalyzes the conversion of soluble fibrinogen to insoluble fibrin, which is crosslinked by factor XIII to form a stable fibrin mesh [15,28].

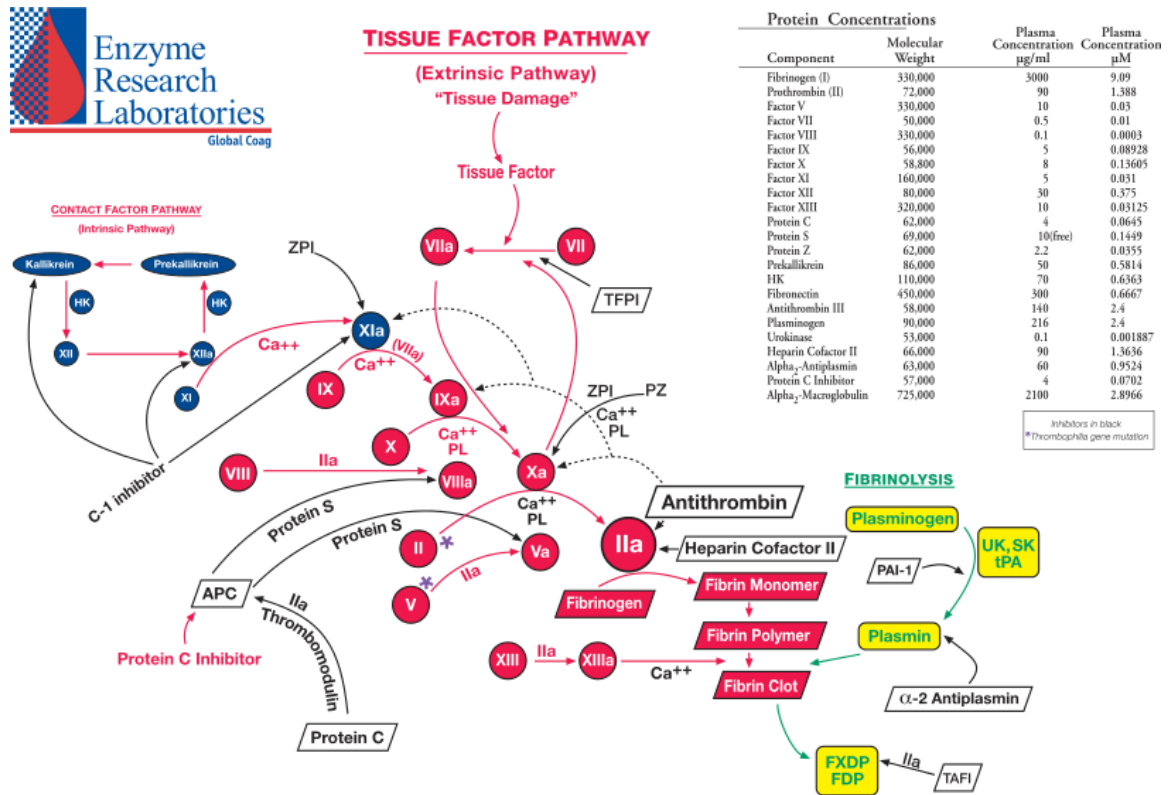


Figure 1. Coagulation cascade showing the intrinsic, extrinsic pathways and fibrinolysis (from: http://www.enzymeresearch.com/CASCADES_2004/images/CASCADE_eri_2007.pdf).

2.2.2.1 Intrinsic and Extrinsic Pathways

The extrinsic pathway is activated by the release of tissue factor from the damaged endothelium of blood vessels, and follows a cascade of reactions that result in the production of activated factor X (FXa) [10].

The intrinsic pathway is initiated by contact activation. When factor XII is adsorbed on a foreign surface, it is activated and converted into FXIIa. FXIIa converts prekallikrein to kallikrein, and factor XI to FXIa, with high molecular weight kininogen (HMWK) as a cofactor in these reactions [10,15]. The cascade of proteolytic reactions

continues from the intrinsic pathway to the common pathway, where factor X is activated and converted to FXa, and FXa converts prothrombin to thrombin. Calcium ions are required for most of the reactions in the coagulation cascade, but not in contact activation [15].

2.2.2.2 Thrombin

Thrombin (factor IIa), a serine protease with a molecular weight of 37 kDa, is a key enzyme in the regulation of coagulation and hemostasis, mainly via its activity in the conversion of fibrinogen to fibrin. It also converts FXIII to FXIIIa, which crosslinks fibrin polymers to stabilize the clot [28]. Thrombin also activates factors V, VIII, and XI to promote its own formation from prothrombin through positive feedback [29]. In addition, thrombin activates platelets, causing adhesion and aggregation of platelets to fibrin within the clot [30].

2.2.2.3 Platelets

Platelets also play an integral role in haemostasis and thrombosis, primarily by forming platelet aggregates that are held together by fibrin polymers, making up the body of the “clot” that preserves the integrity of the vascular wall (haemostasis) or of the thrombus that causes device failure [28]. There are several interactions between platelets and clotting factors in the coagulation cascade [28]. For example, fibrinogen and thrombin contribute to platelet activation, adhesion and aggregation [15]. Once activated, platelets may release additional active agents including fibrinogen, HMWK and von

Willebrand factor [28]. In addition, activated platelets promote the activation of factor X to FXa and the conversion of prothrombin to thrombin [15]. Platelet aggregates formed on a surface in the bloodstream can break away or embolize, potentially causing damage at downstream locations (brain, lung, coronary arteries).

2.3 Inhibition of Coagulation

2.3.1 Heparin

Since thrombin plays a central role in coagulation, the inhibition of thrombin is a common property of anticoagulants. Heparin is used clinically as an anticoagulant, and has been shown to be effective in the prevention and treatment of venous thrombosis, pulmonary embolism, and myocardial infarction in patients with unstable angina [31]. Heparin is a highly sulfated and strongly anionic polysaccharide which belongs to the class of glycosaminoglycans, a family of linear macromolecules made up of repeating units of uronic acid-hexosamine disaccharides, with similar functional groups. It is highly polydisperse with molecular weights in the 3-30 kDa range and an average value of 12-15 kDa [30–33]. Unfractionated heparin (UFH) is a commonly used heparin product with an average molecular weight in the 12-16 kDa range [31].

2.3.1.1 Heparin as an Anticoagulant

Heparin promotes anticoagulation by binding to antithrombin (AT, molecular weight 58 kDa), thereby greatly increasing the rate of inhibition of thrombin by AT (Fig.

2) [35]. Heparin first binds and induces a conformational change in AT to increase its affinity for thrombin [33]. The heparin/AT complex binds thrombin to form a ternary complex [33]. As a result, AT is cleaved at its reactive centre near the C-terminal by thrombin, leaving the larger fragment of AT to be covalently and irreversibly bound to thrombin via an ester bond. The resulting product is referred to as the thrombin-antithrombin (TAT) complex [33]. In these reactions, heparin acts as a catalyst and dissociates from the complex after thrombin is inactivated [33]. Heparin can increase the rate of reaction between thrombin and AT by at least 1000-fold [30,33]. In the absence of heparin, the inactivation of coagulation by AT occurs at a much lower rate [10].

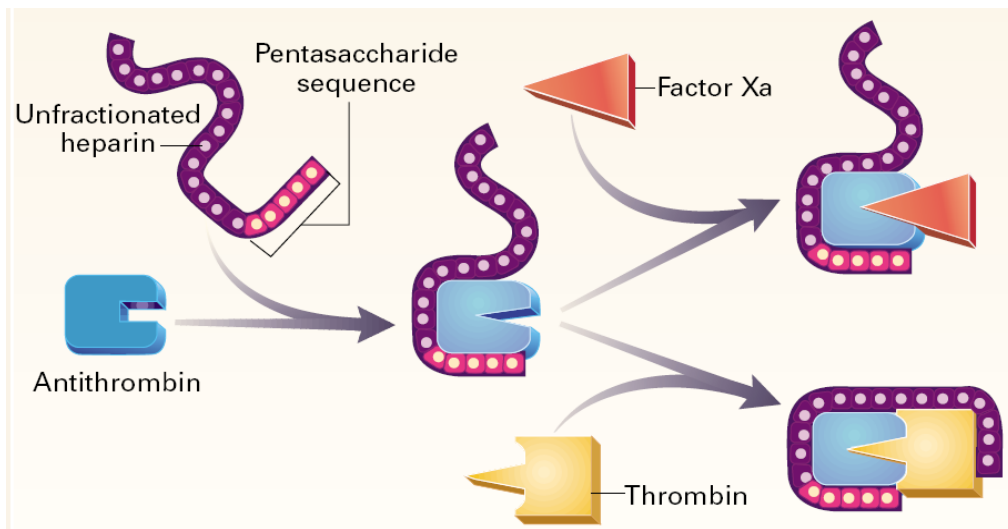


Figure 2. Schematic illustrating the inhibition of factor Xa and thrombin by antithrombin (AT) catalyzed by unfractionated heparin (UFH) (With permission from [34]).

It was found that only heparin molecules with a specific pentasaccharide sequence are able to bind AT with high affinity; approximately one-third of unfractionated heparin (UFH) molecules contain this sequence [30]. The structure of the pentasaccharide

sequence is shown in Fig. 3. The negatively charged groups in the sequence interact specifically with certain positively charged lysine and arginine residues in AT [37].

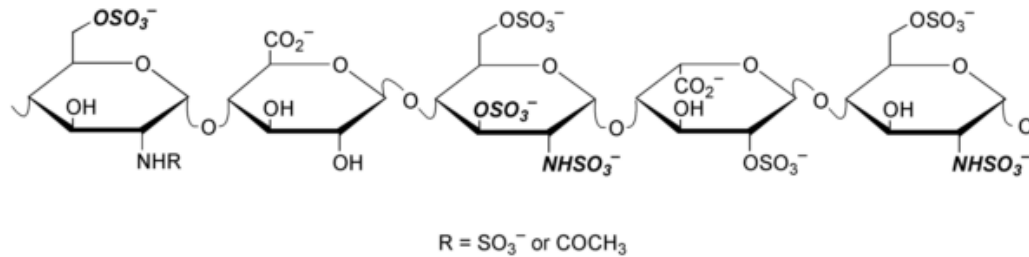


Figure 3. Structure of the pentasaccharide sequence in heparin (adapted from [36]).

2.3.1.2 Heparinized Surfaces

Heparin has been investigated extensively as a surface modifier to improve blood compatibility. Heparinized surfaces have been prepared by ionically or covalently attaching heparin to polymer surfaces [38]. Since it is strongly negatively charged, heparin can be bound to positively charged surfaces through ionic interactions. Gott et al. developed one of the earliest heparinized surfaces in 1963, by coating graphite with benzalkonium chloride, a cationic surfactant, and then attaching heparin. The resulting graphite-benzalkonium-heparin material was used as a coating on prosthetic heart valves [39]. This modification strategy is the basis for the more recent Duraflo IITM surface (Baxter Healthcare Corporation, Irvine, CA) [18,39].

One of the challenges of immobilizing heparin on a surface is that the pentasaccharide sequence must remain intact and accessible in order to preserve the functional activity of the immobilized heparin molecules. Ideally, the heparin chain should be directed away from the surface so that the pentasaccharide sequence is exposed

to allow AT binding. For ionically bound heparin, multiple ionic interactions are required to retain heparin at the surface, since the interactions are relatively weak [11]. While multiple ionic interactions may improve the stability of the heparin, the functional activity of the coating may be compromised if the pentasaccharide sequence is poorly exposed or sterically hindered [11]. Heparinized surfaces based on ionic interactions may also be described as heparin-releasing surfaces, since the bound heparin elutes from the surface into the blood over time by ionic exchange and acts as an anticoagulant in the blood. However the exposed cationic surface may induce platelet adhesion leading to thrombus formation, making such surfaces unsuitable for long term applications [38,40].

Immobilizing heparin on surfaces by covalent attachment should, in principle, produce a more stable coating that is more suitable for long term use. The Carmeda® BioActive Surface (CBAS, Medtronic, Minneapolis, MN) is prepared by so-called end-point covalent immobilization of heparin. It is claimed that this preserves the structural integrity and function of the pentasaccharide sequence [11]. The substrate surface is primed by adsorbing layers of positively and negatively charged polymers resulting in functionalization of the surface with primary amino groups [11,41]. Heparin is modified by formation of an aldehyde group at the chain end, and the aldehyde groups react with the amino groups on the surface to form a Schiff's base which is then stabilized by reduction [11,41].

Heparinized surfaces have been shown to be less thrombogenic than unmodified control surfaces, with increased clotting time, reduced platelet adhesion, reduced complement activation and reduced leukocyte activation [11,40,42]. Heparinized surfaces

have been used clinically in devices such as stents, heart valves, oxygenators, vascular grafts, catheters, and ventricular assist devices [40]. For example, heparinized extracorporeal circuits were utilized in cardiac surgery involving cardiopulmonary bypass. The use of a more thromboresistant circuit allows for lower systemic heparin dose, with fewer bleeding complications and a reduced need for blood transfusions [18,43]. These factors improved the clinical outcome for patients by reducing ventilator support time and length of hospital stay [43].

2.3.1.3 Limitations of Heparin

Unfractionated heparin (UFH) has a short half-life (18 min to 1h) in the circulation [30]. After entering the bloodstream heparin binds to a variety of plasma proteins, platelets, blood cells and endothelial surfaces, thus removing it from circulation, lowering its bioavailability and producing a variable anticoagulant response [30,31].

Heparin is unable to inhibit surface-bound coagulation factors, including fibrin-bound thrombin and phospholipid-bound factor Xa [44]. After thrombin converts fibrinogen to fibrin, it remains trapped within the fibrin clot [29]. Heparin is unable to inhibit fibrin-bound thrombin because it forms a ternary complex with thrombin and fibrin, and is then unavailable to bind AT. Heparin in this state may actually increase thrombin adsorption to the fibrin clot and promote coagulation [29].

Exposure of blood to heparin can also cause heparin-induced thrombocytopenia (HIT), which is characterized by lowered platelet count, platelet aggregation and activation of coagulation, increasing the risk of thrombosis [10,31].

2.3.2 Antithrombin-Heparin (ATH) Covalent Complex

2.3.2.1 ATH as an Anticoagulant

ATH is a novel anticoagulant developed to overcome the limitations of UFH, with a longer half life, higher inhibition rates and the ability to inhibit coagulation by both direct and catalytic heparin-based mechanisms [30]. The method of preparing ATH ensures that the heparin chain in each complex has at least one pentasaccharide sequence, and some have two or more sequences [44]. (See below for more details.)

Since the AT portion of ATH is covalently linked to the heparin portion, the AT is therefore pre-activated to allow rapid thrombin or factor Xa inhibition directly. In addition, the heparin portion of ATH can bind AT in the blood to inhibit thrombin or factor Xa by the usual catalytic mechanism. ATH inhibits coagulation factors faster than UFH because the rate-limiting step of binding AT is removed [44]. ATH can also inhibit fibrin-bound thrombin at a faster rate than heparin because the covalent linkage between AT and heparin in ATH prevents the formation of the heparin-thrombin-fibrin ternary complex [44].

ATH has an intravenous half-life that is longer than heparin and more similar to that of AT (the half-life of heparin in humans ranges from 18 min to 1h, but the half-life of AT is 2.7 days) [30,45]. ATH is a larger molecule than heparin due to its polypeptide component, resulting in greater steric hindrance when approaching other molecules such as proteins. Consequently, ATH shows less non-specific binding to endothelial and cell surfaces, and is able to stay in the circulation longer than heparin [30].

2.3.2.2 Synthesis of the covalent ATH complex

The synthesis of ATH involves the reaction of AT with heparin, in which the protein binds covalently to the aldose-terminating polysaccharide [35]. AT is incubated with a 200 molar excess of UFH in PBS at 40°C for 14 days [14]. The choice of incubation temperature is important for optimizing the yield of ATH; thus it was shown that incubation at 37°C resulted in a yield of about 5%, whereas at 40°C a yield of about 50% was achieved [30]. A 200 molar excess of UFH is necessary because only one-third of UFH molecules have a pentasaccharide sequence (Fig. 4), and only about 10% contain a free terminal aldose to form a covalent bond with AT [30].

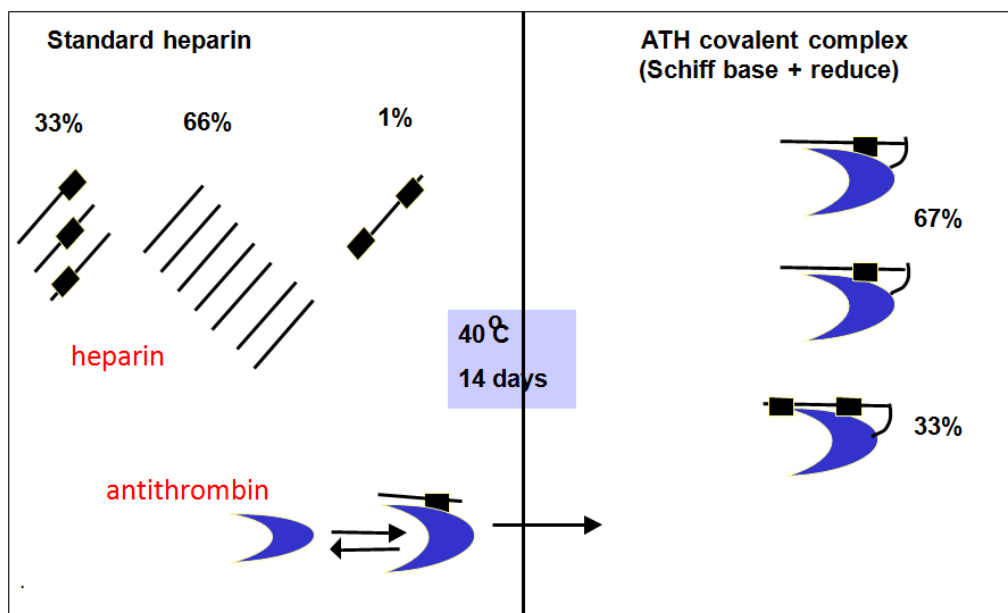


Figure 4. Schematic showing the synthesis of the ATH covalent complex from standard heparin, rectangular blocks on the heparin chains represent the pentasaccharide sequence, curve at end of heparin chain to blue AT molecule represents the covalent keto-amine linkage between aldose aldehyde and N-terminal amine (Courtesy of L. Berry, McMaster University).

When AT is incubated with UFH under the above reaction conditions, it initially binds to heparin non-covalently through the pentasaccharide sequence (Fig. 4) [46]. In a much slower reaction, a Schiff base (imine) forms by reaction of ϵ -amino groups on the lysine residues in AT with the aldehyde group on the aldose terminus of heparin (Fig. 5) [30]. In the presence of a free hydroxyl group on C2 of the terminal sugar, Amadori rearrangement occurs between the groups on C1 and C2 of the sugar, converting the imine with a hydroxyl group to an amine with a ketone group (Fig. 5) [44]. After the 14 day incubation, NaBH_3CN is added to reduce any Schiff base not stabilized by Amadori rearrangement [44].

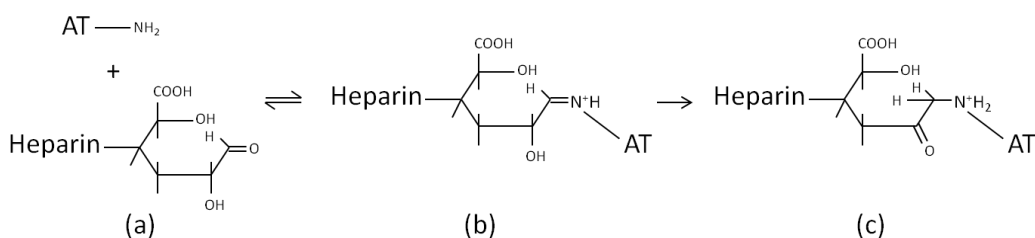


Figure 5. Synthesis of the covalent ATH complex via Schiff base formation (a to b) and Amadori rearrangement (b to c) (adapted from [47]).

Several protein purification steps are needed to remove unreacted AT and heparin. Butyl-agarose chromatography is used to remove unbound heparin, followed by DEAE Sepharose chromatography to remove unbound AT [14,44]. This procedure, developed by Chan et al., produced a pure 1:1 complex of heparin and AT, with a yield of 50% based on conversion from AT; this is much higher compared to previous work by other groups [44].

2.3.2.3 Surfaces modified with ATH

Compared to heparin, AT has more functional groups that can be used for covalent bonding to surfaces. For example ATH can be immobilized using the ϵ -amino groups on the lysine residues in AT, with the heparin portion free to inhibit coagulation factors [30].

Sask et al. immobilized ATH covalently on gold and polyurethane using a PEO spacer, and compared the anticoagulant potential of the ATH-modified surfaces to analogous heparinized surfaces [13,48,49]. On both gold and polyurethane, it was shown that the ATH-modified surfaces had enhanced anticoagulant activity compared to analogous heparin-modified surfaces. *In vitro* experiments indicated lower non-specific protein adsorption, higher AT adsorption from plasma, greater anti-factor Xa activity, lower platelet adhesion, and prolonged plasma clotting time [13,48,49].

Klement et al. reported on polycarbonate urethane endoluminal grafts covalently grafted with ATH [50]. The ATH-coated grafts demonstrated high anticoagulant activity based on thrombin inhibition *in vitro* [50]. For *in vivo* testing, the uncoated and coated grafts were inserted into the jugular vein of rabbits. After three hours, it was observed that thrombus deposition was much lower in the ATH-coated grafts than in the uncoated ones [50].

Du et al. coated ATH onto polyurethane catheters and evaluated their anticoagulant activity *in vivo* using a rabbit model [51,52]. Uncoated, heparin-coated and ATH-coated catheters were inserted into the rabbit jugular vein, and it was found that the

uncoated and heparin-coated catheters clotted in less than 8 days after insertion, whereas the ATH-coated catheters resisted clotting and remained patent for >100 days [52].

2.4 Silicones

2.4.1 Silicone Structure

Polysiloxanes (silicones) are a class of synthetic polymers with an alternating silicon-oxygen backbone, and two organic groups bonded to each silicon atom [15]. The most common silicone elastomer is polydimethylsiloxane (PDMS), in which the two organic groups are methyl (-CH₃) [15]. Fig. 6 shows the structure of a trimethylsiloxy terminated PDMS.

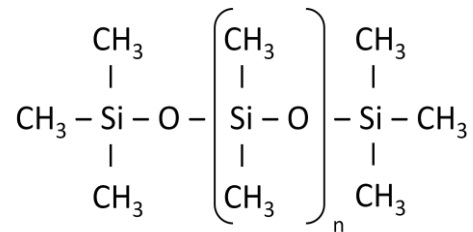


Figure 6. Trimethylsiloxy terminated polydimethylsiloxane (PDMS).

2.4.2 Silicone in Biomedical Applications

Silicone has a long history of use as a biomaterial due to its reasonably good biocompatibility, low toxicity, good mechanical properties, and good thermal and chemical stability [5,6,8]. It is also relatively inexpensive, and easy to process. It has therefore been used in a wide range of biomedical products, devices, implants, and prostheses [8]. Examples include medical-grade tubing, medical adhesives, mammary prostheses, artificial skin, maxillofacial reconstruction, replacement oesophagus, and transdermal drug delivery patches [6,53]. In particular, silicone is useful for ophthalmic

applications due to its high optical transparency and oxygen permeability. Examples include contact lenses, artificial corneas, and drainage implants for the treatment of glaucoma [6,7,54]. In blood-contacting applications, silicone has been used in catheters, blood pumps, extracorporeal oxygenators, pacemaker leads, prosthetic heart valves, and arteriovenous shunts used by hemodialysis patients [3,6].

2.4.3 Surface Modification of Silicone

Since silicone is strongly hydrophobic and therefore strongly protein-adsorbent, surface modification is used to make the surface more hydrophilic and reduce non-specific adsorption of proteins and adhesion of cells. Increased hydrophilicity also improves lubricity for microfluidics applications. The silicone surface must first be primed or activated to allow the introduction of functional groups [55].

PDMS can be modified with PEG by physical adsorption or covalent attachment. For physical adsorption of PEG, PDMS was first treated by oxygen plasma to create a negatively charged surface, followed by incubation with the positively charged copolymer, poly(L-lysine)-graft-PEG [9]. In another technique PEG copolymers were blended with PDMS pre-polymer and became trapped in the PDMS matrix after curing [9].

For covalent attachment of PEG, PDMS was initially functionalized with Si-H groups under acid catalysis or argon plasma conditions (Fig. 7), followed by a platinum-catalyzed hydrosilylation reaction (Fig. 8). This is an addition reaction between Si-H and allyl groups to create Si-C bonds, and is a common method to replace the methyl groups

on PDMS with other R groups such as PEG [6,57,58]. The immobilized PEG was shown to inhibit non-specific protein adsorption, and could also act as a spacer for the attachment of other molecules such as heparin as an anticoagulant, or ϵ -lysine as a profibrinolytic agent [4,55]. Heparin can also be directly immobilized on PDMS by converting the Si-H groups to primary amino groups for heparin attachment [58]. PDMS has also been functionalized with trypsin, a proteolytic enzyme, to resist protein adsorption and cell adhesion in shunts [59]. Nitric oxide (NO)-releasing silicone was also developed to improve its blood compatibility (NO is produced by the endothelium to regulate haemostasis by reducing platelet activation) [60]. For this purpose silicone was impregnated with copper particles to catalyze the release of NO from NO-donating molecules in blood [60,61].

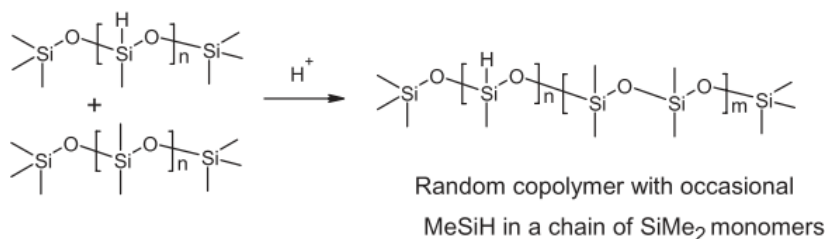


Figure 7. Functionalization of PDMS with SiH groups (adapted from [24]).

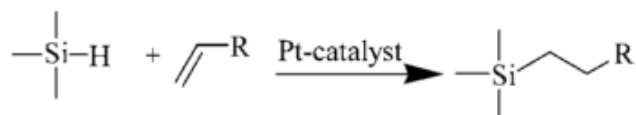


Figure 8. Hydrosilylation reaction involving a Si-H group and a terminal double bond catalyzed by a platinum catalyst [56].

2.5 Thromboelastography (TEG)

Thromboelastography is an experimental method used to characterize the coagulant state of a blood or plasma sample *in vitro* [62]. In TEG analysis the viscoelastic changes that occur during coagulation are monitored and analyzed [62]. Results are presented in the form of a TEG curve (Fig. 11), which provides information on the initiation of clotting, the formation of the clot and its stability [62,63]. TEG is commonly used in clinical settings to monitor the coagulation patterns of patients, to assess bleeding risks and the maintenance of haemostasis [62,63]. Examples include the assessment for hemorrhage or thrombosis following cardiopulmonary bypass, liver surgery, or organ transplant [63]. It is also used for assessing patients with haemophilia or hypercoagulable conditions [63,64]. In research settings TEG is used to evaluate the efficacy of anticoagulants, anti-fibrinolytic drugs, and platelet-inhibiting drugs [62]. Very recently it has also been used to characterize the coagulant nature of biomaterials [64,65].

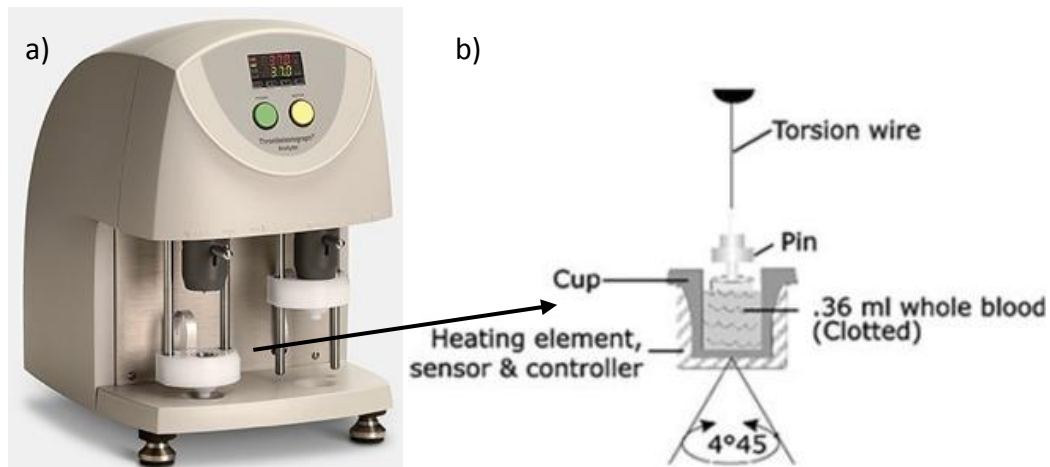


Figure 9. (a) The TEG 5000 Thromboelastograph Hemostasis Analyzer System (Haemoscope Corporation, Niles, IL) (b) TEG cup and pin assembly that sits in the (white) holder during analysis (adapted from [66]).

2.5.1 Principle of Thromboelastography

A blood or plasma sample (typically 0.36 mL) is added to the TEG cup, which is placed in a holder on the machine (Fig. 9a). Coagulation is initiated, typically by adding CaCl_2 to citrated blood or plasma. A pin is suspended in the sample by a torsion wire. The TEG cup is oscillated in the horizontal plane, and the torque on the stationary pin is measured by the torsion wire (Fig. 9b) [62]. When the clot begins to form, the torque on the oscillating cup is transmitted to the pin, and the movement of the pin is measured continuously. The pin's movement which depends on the torque generated, is correlated with the mechanical strength of the developing clot [62]. When the clot has fully formed, the pin rotates synchronously with the cup.

The characteristics of clotting are measured throughout the test via the torque and displayed as a curve (Fig. 10). The curve, reflecting the different stages of coagulation, provides information on clot formation and properties (Fig. 10, Table 1).

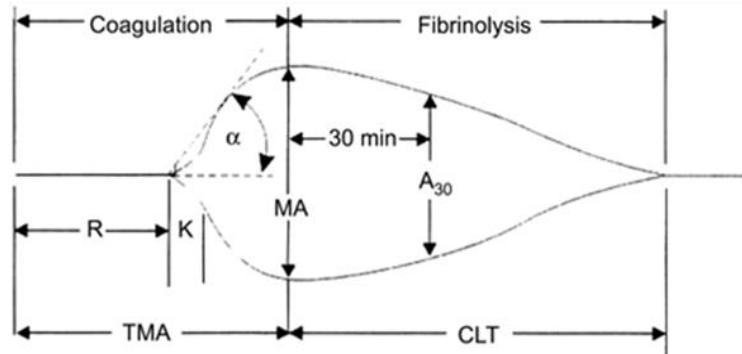


Figure 10. Reference diagram for TEG curves. Parameters in figure are explained in Table 1. The x-axis is time (min); the y-axis is distance in mm reflecting clot strength (adapted from [62]).

Table 1. Explanation of parameters in TEG curves [62].

Parameter	Units	Represents	Explanation (see Fig. 11)
Reaction time (R)	Min	Speed of clot formation	R is the time for the curves to diverge with an amplitude of 2 mm, as initial fibrin formation is detected.
Coagulation time (K)	Min	Speed of clot development	K is the period from the start of clot formation to when the curves diverge with an amplitude of 20mm. K is shortened by increased fibrinogen level and platelet function. K is undefined if the amplitude does not reach 20mm.
α angle	Degrees	Rate of clot development	α is the angle between the horizontal and a tangent on the TEG curve that intersects the point when the two curves diverge, it measures the speed of fibrin cross-linking and polymerization. α increases with increasing fibrinogen level and platelet function.
Maximum amplitude (MA)	mm	Maximum clot strength	The maximum amplitude between the two curves; a measurement of maximum strength of the developed clot.

2.5.2 Application of TEG in the Evaluation of Biomaterials

TEG is typically used for the analysis of liquid samples, such as blood from patients to assess coagulation state and activity or efficacy of anticoagulants. Given the convenience and the reliability of the assay, it should be beneficial to use TEG to study blood-material interactions and evaluate the thrombogenicity of different materials. TEG characterizes clotting by measuring the viscoelasticity of the sample as it clots, and may be more sensitive than clotting assays that rely on absorbance or turbidity measurements. A plasma recalcification assay that is commonly used to determine clotting time was described previously. Surfaces are incubated with re-calcified plasma in a 96-well microtitre plate, and clotting time is determined based on the change in turbidity of the plasma sample as it clots [48,67]. A limitation of this assay is that the presence of the biomaterial in the well may block the path of the light through the sample, giving rise to

errors and likely decreasing the sensitivity of the assay. In comparison, TEG is more reliable and more sensitive because small changes in viscoelastic properties can be detected during clotting, and the presence of the biomaterial is irrelevant.

In addition to the determination of clotting time, TEG provides additional information such as rate of clot formation, clot strength and clot stability. TEG can be used to analyze plasma samples, including platelet-poor and platelet-rich plasmas. Studies of coagulation factor-deficient plasmas may provide information on specific coagulation pathways, and on the interactions of biomaterials with specific blood components [64]. TEG can be used to study blood-material interactions as coagulation occurs, including the interactions of platelets and blood cells. However, the TEG procedure must be modified to accommodate the analysis of solid samples, and surface preparation for TEG analysis may be challenging.

In a recent study, TEG was used to evaluate and compare the thrombogenicity of several biomaterials, including polytetrafluoroethylene (PTFE), a polyurethane, polystyrene and Tygon; the biomaterials were incubated with blood and the blood was then subjected to TEG analysis [65]. Of all the biomaterials, PTFE was shown to have the longest reaction time (R) and therefore the lowest thrombogenicity. This result could be expected given that PTFE is commonly used in vascular grafts [65]. In addition, TEG was used to study the effects of “passivating” surfaces with endothelial cell (EC) layers to imitate the natural vascular endothelium. Polystyrene-EC showed increased clotting time (R) and coagulation time (K) compared to unmodified polystyrene, demonstrating that the EC layer effectively reduced the thrombogenicity of the surface [65]. Peng et al. reviewed

the use of TEG for the study of blood-soluble polymers, blood-insoluble polymers, hydrogels, and ceramic biomaterials [64]. Blood-soluble polymers such as dextran were mixed with the blood during analysis, and blood-insoluble polymers were either prepared as microparticles or dip-coated onto the TEG cup [64].

3. MATERIALS AND METHODS

3.1 Materials

Sylgard® silicone elastomer kit was purchased from Dow Corning (Midland, MI). Polyhydromethylsiloxane was purchased from Gelest (Morrisville, PA). α -allyl- ω -hydroxy-PEG was obtained as a gift from Clariant (Frankfurt, Germany). Trifluoromethanesulfonic acid ($\text{CF}_3\text{SO}_3\text{H}$), Karstedt's platinum catalyst (2–3 wt% in xylene), isopropanol, anhydrous methanol, anhydrous hexane, N,N'-disuccinimidyl carbonate (DSC), sodium periodate (NaIO_4) and sodium borohydride (NaBH_4) were purchased from Sigma Aldrich (Oakville, ON). Triethylamine (TEA, 99%) and anhydrous acetonitrile were purchased from EMD Chemicals (Gibbstown, NJ).

Fibrinogen was purchased from Enzyme Research Laboratories (South Bend, IN). AT was purchased from Affinity Biologicals Inc. (Ancaster, ON). Heparin sodium salt from porcine intestinal mucosa was purchased from Sigma Aldrich (Oakville, ON). ATH was prepared by incubating AT and heparin at 40°C for 14 days, followed by purification with butyl-agarose to remove unreacted heparin, and with DEAE Sepharose to remove unreacted AT as described previously [68].

Na^{125}I was from the McMaster Nuclear Reactor (Hamilton, ON). Iodogen iodination reagent was purchased from Pierce Biotechnology (Rockford, IL). Slide-A-Lyzer cassettes were purchased from Pierce Biotechnology (Rockford, IL). Platelet poor acid citrate dextrose (ACD) plasma was prepared from whole blood collected from

multiple healthy donors. The collected plasma was aliquoted and stored at -70°C . TEG cups and pins were purchased from Haemoscope Corporation (Niles, IL).

3.2 Methods

3.2.1 Surface Preparation

PDMS films were prepared using the Sylgard® silicone elastomer kit by mixing the elastomer base with the curing reagent in a 10:1 ratio. The mixture was poured into a Petri dish, degassed for 30 min at 80°C , and cured at room temperature for 2 days. The resulting film, about 0.5 mm thick, was punched into 6 mm diameter discs.

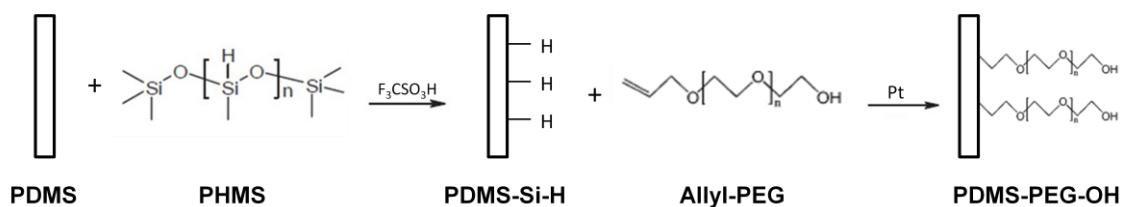


Figure 11. Reaction scheme for grafting PEG on PDMS.

To introduce Si-H groups into the PDMS surface, PDMS discs were washed in 10 mL of methanol for 30 min, and then reacted with 3 mL of polyhydromethylsiloxane (PHMS) in 5 mL of anhydrous methanol [24]. 50 μL of trifluoromethanesulfonic acid ($\text{CF}_3\text{SO}_3\text{H}$) was added as catalyst (1 vol% in methanol) and the system reacted for 30 min at room temperature [24]. Surfaces were rinsed sequentially in 10 mL methanol, 10 mL hexane and 10 mL methanol (10 minutes each) to remove residual reactants, and dried under vacuum for 1 hour [24].

PEGs of molecular weight 350 and 550 kDa were grafted to the modified PDMS by reaction of Si-H groups on the surface with allyl groups of α -allyl- ω -hydroxy-PEG. Surfaces were reacted with 4 g of PEG (62.5 wt%) in 2.4 g of isopropanol and 60 μ L of Karstedt's platinum catalyst for 18 h at room temperature [55]. They were then rinsed with acetone and water, and dried under vacuum overnight [55].

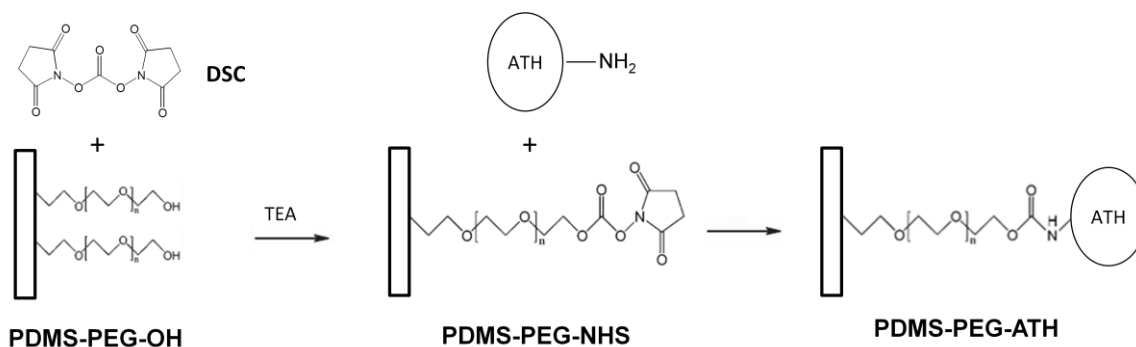


Figure 12. Reaction scheme for immobilizing ATH on PDMS previously functionalized with PEG.

PEG-modified surfaces were rinsed with 5 mL of anhydrous acetonitrile for 30 min. N,N'-disuccinimidyl carbonate (0.0512 g) was dissolved in 4 mL of anhydrous acetonitrile, 27.4 μ L of triethylamine was added as catalyst, the PEG-modified surfaces were added and the vial was sealed with nitrogen and reacted for 6 h at room temperature. The hydroxyl end groups of PEG were thus converted to N-hydroxysuccinimide (NHS) groups [69]. Surfaces were then rinsed 3 times with anhydrous acetonitrile (5 min each time) and then briefly with water.

ATH and heparin were attached to the PEG-NHS surface by reaction of NHS with amino groups of ATH and heparin. ATH (0.1 mg/mL) or heparin (1 mg/mL) were incubated with the surfaces in phosphate buffered saline (PBS) overnight at 4°C [70]. The

surfaces were treated with 2M NaCl for 3 h at room temperature prior to use to remove loosely bound ATH or heparin, and rinsed with PBS [70].

3.2.2 Water Contact Angles

Advancing and receding water contact angles were measured with a Ramé-Hart NRL C.A. goniometer (Mountain Lakes, NJ) using the sessile drop method with Milli-Q water.

3.2.3 X-ray Photoelectron Spectroscopy (XPS)

Surfaces were analyzed by XPS at Surface Interface Ontario (University of Toronto) using a Thermo Scientific K-Alpha XPS spectrometer with a monochromatic Al source and a spot size of 400 μm . Elemental compositions of the surfaces were determined from low resolution scans for C, O, N, S and Si. The samples were run at a take-off angle of 90° relative to the surface. Data processing was performed with the Advantage Data Analysis Software.

3.2.4 Protein Radiolabelling

3.2.4.1 Iodogen Method

AT and ATH were radiolabelled with Na^{125}I using the Iodogen method [71]. 100 μg of protein and 5 μL of Na^{125}I were added to a vial coated with 10 μg of Iodogen iodination reagent and reacted for 15 min. The reaction mixture was transferred to a

Slide-A-Lyzer cassette and dialyzed overnight with three changes of buffer to remove unbound radioisotope.

3.2.4.2 Iodine Monochloride Method

Fibrinogen was radiolabelled with Na¹²⁵I using the iodine monochloride method [71]. 10 mg of fibrinogen was added to 22.3 µL of ICl reagent, 0.24 mL of glycine buffer, and 5 µL of Na¹²⁵I. The reaction mixture was passed through a column containing AG 1X4 anion exchange resin to remove unbound radioisotope.

3.2.4.3 Determination of Free Iodide

Free iodide refers to the percentage of unbound radioactive iodide that remains after the radiolabelling process and subsequent dialysis or ion exchange. To determine free iodide, trichloroacetic acid (20% w/v in water) was added to the radiolabelled protein solution to precipitate the protein, and the radioactivity of the supernatant was determined. Free iodide was expressed as the fraction of the radioactivity of the supernatant divided by the total radioactivity of the labelled protein solution. Free iodide contents for labelled fibrinogen, AT and ATH were all below 4%.

3.2.5 Protein Adsorption Experiments

For experiments to measure the quantity of protein adsorbed from buffer, surfaces were incubated in a solution of either ATH at 0.1 mg/mL or fibrinogen at 1 mg/mL, where 2% of the ATH or fibrinogen was radiolabelled and the other 98% was unlabelled.

For plasma experiments with AT or fibrinogen, radiolabelled protein was added to the plasma at a concentration corresponding to 10% of the normal endogenous level.

For both buffer and plasma experiments, surfaces were incubated in the medium for 3 h, rinsed and transferred to 2 % sodium dodecyl sulfate (SDS) solution to remove loosely bound proteins. The quantity of protein adsorbed was calculated from the radioactivity of the surfaces before and after SDS incubation, measured using a Wizard Automatic Gamma Counter (PerkinElmer, Waltham, MA).

3.2.6 Sodium Dodecyl Sulfate–Polyacrylamide Gel Electrophoresis (SDS–PAGE) and Western Blotting

Sixteen discs of each surface were incubated in plasma for 3 h, rinsed with PBS three times to remove residual plasma, and incubated in 250 μ L of 2% SDS overnight to elute the adsorbed proteins. Eluates were run on reduced SDS-PAGE (12% gels) to separate the proteins. Proteins were transferred from polyacrylamide gels to polyvinylidene fluoride (PVDF) membranes using the iBlot® 7-Minute Blotting System (Invitrogen, Israel, WV). Membranes were incubated in a solution with non-fat dry milk to block unbound sites, then exposed to primary antibodies at a dilution of 1:1000, and secondary antibodies conjugated to alkaline phosphatase at a dilution of 1:1000 to detect specific proteins.

3.2.7 Destruction of the Pentasaccharide Sequence in Heparin

To test the specificity of plasma interactions with the modified surfaces, experiments were conducted in which the heparin moieties were selectively degraded.

ATH- and heparin-modified surfaces were incubated with 0.1M NaIO_4 for 18 h in the dark, rinsed with water, incubated in 1M NaBH_4 for 5 h, and rinsed with water before use [51]. These reactions are illustrated in Fig. 13. The pentasaccharide sequence in heparin is shown in Fig. 13a, and IO_4^{4-} converts the two hydroxyl groups on the non-sulfonated glucuronic acid to aldehyde groups (Fig. 13b), opening the ring structure. NaBH_4 reduces the aldehyde groups to hydroxyl groups, and the resulting structure in Fig. 13c is unable to bind AT for anticoagulation.

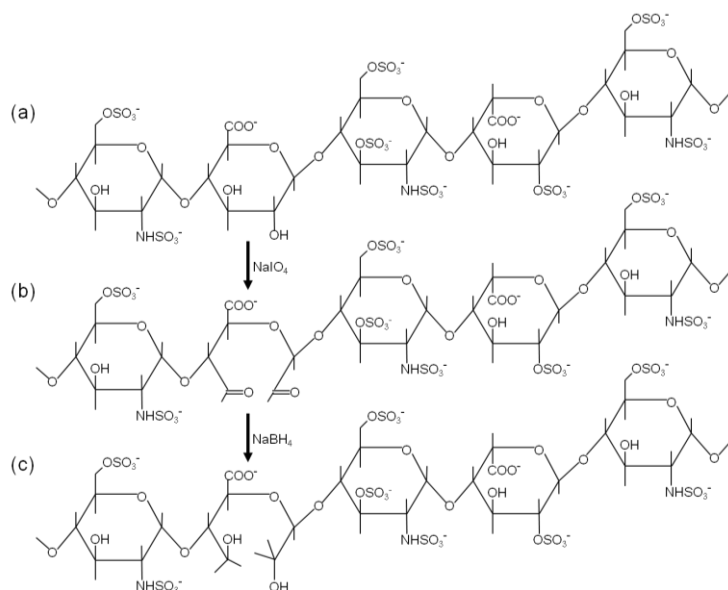


Figure 13. Destruction of the Pentasaccharide Sequence in Heparin by chemical treatment with NaIO_4 and NaBH_4 (Courtesy of L. Berry, McMaster University).

3.2.8 Thromboelastography (TEG)

The objective of the TEG experiments was to provide data on the anticoagulant potential of PDMS modified with ATH by covalent immobilization via a PEG spacer. Due to the complexity of the surface modification reactions in covalent immobilization

(see section 3.2.1), ATH-modified PDMS prepared by simple physical adsorption from solution was used in preliminary experiments to test the utility of the TEG method for evaluation of these materials. The TEG 5000 Thromboelastograph Hemostasis Analyzer System (Haemoscope Corporation, Niles, IL) was used for all TEG experiments (Fig. 9a).

3.2.8.1 TEG Analysis of PDMS Coated with ATH by Physical Adsorption

TEG cups were coated with a thin layer of PDMS by dip-coating. The mixture of pre-polymer and curing agent was added to the TEG cup and the excess was poured out. The cups were then placed in an 80°C oven for 30 min, and held at room temperature for 2 days to complete curing. Since the layer of PDMS on the TEG cups was very thin, the inner volume of the TEG cup remained essentially unchanged. The PDMS-coated cups were incubated with a 0.1 mg/mL solution of ATH in PBS overnight, rinsed with buffer three times, 5 min each, before use.

For TEG analysis, 340 μ L of plasma and 30 μ L of 0.13M CaCl₂ were added to the TEG cup and mixed briefly before initiating the run.

3.2.8.2 TEG Analysis of PDMS Coated with Covalently Bound ATH via PEG spacer

For covalent immobilization of ATH on PDMS via PEG spacer, the PDMS must undergo a series of chemical reactions as described. Therefore, it was necessary to coat the TEG cup with a thicker layer of PDMS, ≥ 0.5 mm, since a thinner coating did not remain intact during solvent exposure in chemical reactions.

To increase the layer thickness PDMS pre-polymer was mixed with the curing agent, degassed in a vacuum oven, and added to the TEG cup. A form-fitting mold was inserted into the centre of the TEG cup and the PDMS polymer mixture was pushed against the walls. This assembly was placed in an 80°C oven for 30 min, and then held at room temperature for 2 days, allowing the PDMS to cure and set according to the shape of the mold, thus coating the inner surface of the cup. The PDMS coatings were separated from the TEG cup and mold, and inserted into 30 mL glass vials for surface modification. The same modification reactions and conditions described in section 3.1 were used, and the reaction volumes were adjusted to ensure that the PDMS coatings were fully submerged in the reaction solutions.

By coating the TEG cup with a thicker layer of PDMS, the inner volume of the TEG cup was slightly reduced. Therefore, the volume of plasma used for TEG analysis was reduced to 165 μL . The plasma was added to the cup along with 15 μL of 0.13M CaCl_2 and mixed briefly before the TEG run was initiated.

3.3 Statistical Analysis

Student's t-test was used to compare data sets for different surfaces. Differences were considered significant at $p < 0.05$. Data are reported as means \pm standard deviation (SD).

4. RESULTS

4.1 Surface Characterization

4.1.1 Water Contact Angles

Water contact angle measurements were taken to assess the hydrophobicity of the surfaces before and after modification with PEG (Fig. 14). The unmodified PDMS was found to be strongly hydrophobic, with an advancing angle of 105° , and a slightly lower receding angle of 97° . The difference between the advancing and receding angles (i.e. hysteresis) on PDMS was low, likely due to the hydrophobicity and smoothness of the unmodified surface [24]. The advancing angle decreased to 76° after modification with PEG350, and to 73° with PEG550, i.e. the PDMS became less hydrophobic. PDMS modified with PEG550 was slightly more hydrophilic than with PEG350, although the difference was not significant ($p>0.05$). The advancing and receding contact angle values of surfaces modified with PEG were consistent with values reported in the literature [4,24]. In comparison to unmodified PDMS, hysteresis was higher on PEG350 and PEG550, probably due to an increase in surface roughness and chemical heterogeneity after surface modification [5].

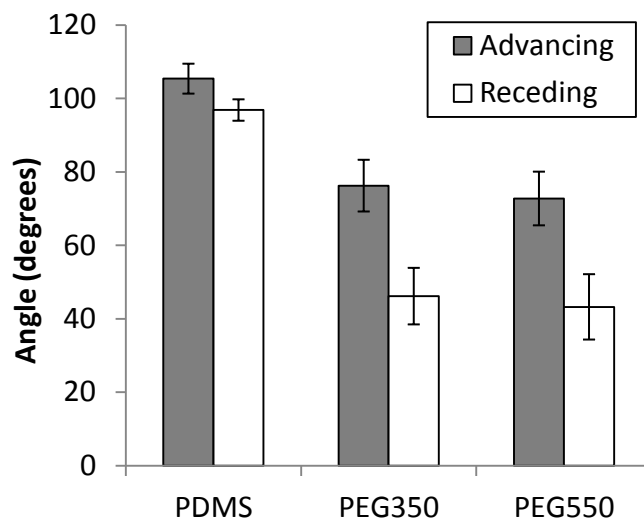


Figure 14. Water contact angles of control PDMS and PDMS modified with PEG350 and PEG550. Advancing and receding angles measured by the sessile drop method. Data are mean \pm SD, $n \geq 12$.

The contact angles of surfaces modified with ATH and heparin (PEG350-ATH, PEG350-heparin, PEG550-ATH, PEG550-heparin) were also measured (data not shown). The advancing and receding angles of PEG350 were similar to PEG350-ATH and PEG350-heparin, which was also observed for PEG550 surfaces. In general, subsequent modifications with ATH or heparin did not significantly change the contact angles of the PEG350 and PEG550 surfaces. Similar studies in the literature have reported a slight increase in contact angles upon conjugation of ATH or heparin to PEG, which was not observed on the PDMS surfaces in this study [13,70]. It is possible that the surface coverage of ATH or heparin was not high enough to result in a significant change in the contact angles.

4.1.2 X-Ray Photoelectron Spectroscopy (XPS)

XPS was used to determine the elemental composition of the surfaces. Typical data are shown in Table 2.

Table 2. Low resolution XPS data (atom %) for PDMS surfaces at 90° take-off angle (data precision, $\pm 5\%$).

Surface	C%	N%	O%	Si%	S%
PDMS	43.7	0.1	25.9	30.3	0.0
PEG550	51.5	0.1	26.4	22.0	0.1
PEG550-ATH	52.8	0.5	26.6	20.0	0.1
PEG550-heparin	50.5	0.1	25.9	23.5	0.1

The carbon and oxygen contents increased following modification with PEG. As a result of PEG-grafting, the PDMS was less “visible” and the silicon content decreased. A small increase in nitrogen content was observed after modification with ATH, corresponding to the protein component of ATH. The changes in elemental composition at each stage of the modifications as determined by XPS are in agreement with those expected, at least qualitatively.

The sulfur content was 0.1% for both PEG550-ATH and PEG550-heparin surfaces, not significantly different from zero and not different compared to PDMS and PEG550 controls. This apparent discrepancy may be due to the relatively low sulfur content of the heparin and therefore of the modified surfaces. Olander et al. were also unable to detect sulfur on PDMS functionalized with primary amines and subsequently coupled with heparin [58].

The sulfur content of standard heparin was estimated to be about 13% by mass, therefore the detection of sulfur with XPS on a heparinized surface may be difficult unless the surface density of heparin is high [72]. Chen et al. reported a slight increase (0.4%) in the sulfur content of PDMS immobilized with heparin through a PEG spacer when the heparin density was determined to be $0.68\mu\text{g}/\text{cm}^2$, which was relatively high [4].

4.2 Protein Interactions

4.2.1 ATH Surface Density and Stability

The purpose of attaching ATH to PDMS is to promote anticoagulant activity at the surface, as expected to occur by the binding of plasma AT. It was important to determine the density of ATH on the surfaces since higher density of ATH is expected to give a greater anticoagulant effect. In addition, it was also important to assess the stability of the ATH surfaces, since the covalent attachment of the ATH complex via PEG was expected to give a more stable surface to provide sustained anticoagulant activity. To assess ATH stability, surfaces were treated with sodium dodecyl sulfate (SDS) a powerful protein eluent.

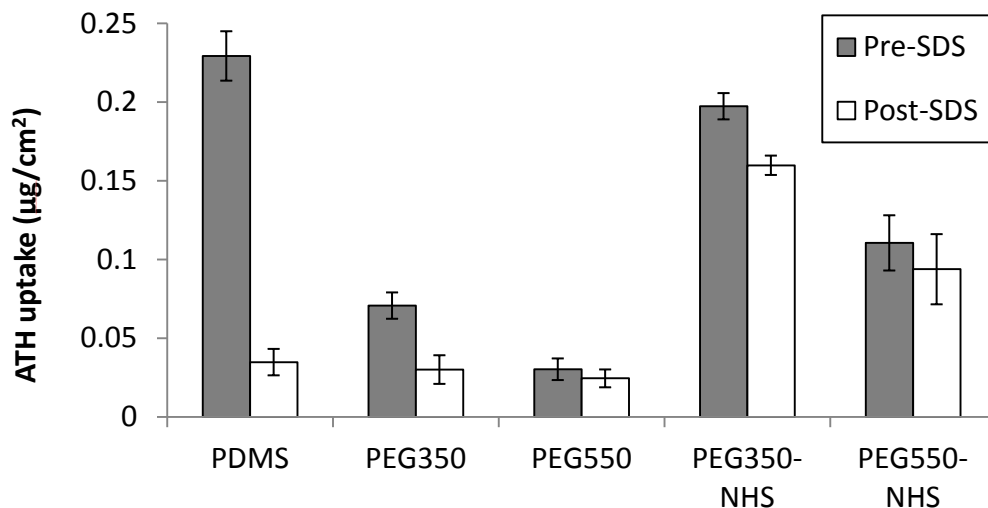


Figure 15. ATH uptake from buffer on surfaces before and after SDS treatment. Surfaces were incubated in ATH (0.1 mg/mL in PBS, 5% radiolabelled) for 3 h. Data are mean \pm SD, n = 3.

As seen in Fig 15, the uptake of ATH on unmodified PDMS was high, with adsorption of $0.23 \mu\text{g}/\text{cm}^2$ corresponding to a monolayer for a species of the size of ATH [13]. However, most of the ATH was elutable by SDS, indicating relatively weak binding as expected for physical adsorption. ATH uptake on the PEG surfaces prior to activation with NHS groups, at $0.1 \mu\text{g}/\text{cm}^2$, was much reduced reflecting the protein resistance of the PEG chains. Likewise, ATH uptake on the non-activated PEG550 surface was low, and even lower than on the non-activated PEG350 surface, again demonstrating protein resistance.

The NHS-activated PEG surfaces took up significant quantities of ATH, and retained $>80\%$ after SDS treatment, suggesting strong (presumably covalent) attachment of ATH (see Fig. 15). Uptake of ATH on the PEG550-NHS surface was lower than on the PEG350-NHS surface, presumably due to the greater protein resistance of PEG550. This

suggests that there may be an optimal balance between the protein resistance of the PEG component and the ability of the surface to bind ATH. The PEG350-NHS surface appeared to be superior to the PEG550-NHS surface in this regard.

4.2.2. Fibrinogen Adsorption from Buffer

To assess the ability of the modified surfaces to resist non-specific protein adsorption fibrinogen adsorption on unmodified and modified PDMS surfaces was measured (Fig. 16). Adsorption, at $1.1 \mu\text{g}/\text{cm}^2$, was highest on unmodified PDMS and significantly lower on all of the modified surfaces, including PEG350, PEG550, PEG350-ATH, and PEG550-ATH ($p < 0.05$).

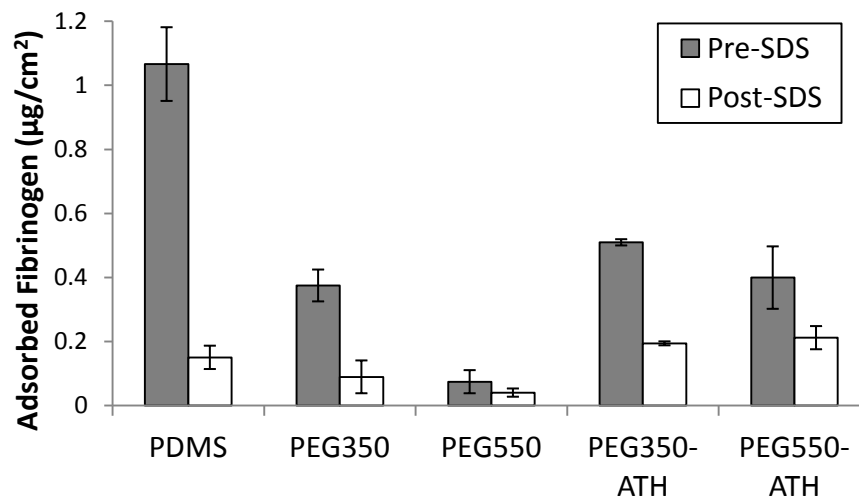


Figure 16. Fibrinogen adsorption to PDMS surfaces modified with PEG and PEG-ATH. Fibrinogen concentration 1 mg/mL in PBS, 2% radiolabelled. Adsorption time 3 h. Adsorbed quantities determined from radioactivity before and after incubation in SDS overnight. Data are mean \pm SD, n = 3.

The greatest protein resistance was seen on the PEG550 surface, with a 93% reduction compared to PDMS, and adsorption of less than $0.1 \mu\text{g}/\text{cm}^2$ (Fig. 16). PEG550 showed significantly greater protein resistance compared with PEG350 ($p < 0.05$), likely due to the longer PEG chains [73]. Even after the immobilization of ATH, fibrinogen adsorption on PEG550-ATH was significantly lower than on PEG350-ATH ($p < 0.05$).

Since ATH was attached to the NHS groups at the distal end of the PEG chains, the ATH component could potentially reduce the protein resistance of the PEG. Fibrinogen adsorption on PEG350-ATH and PEG550-ATH was not as low as on PEG350 and PEG550 (Fig. 16), but the difference was significant only on the more protein resistant PEG550 surface ($p < 0.05$). This was also observed on similar surfaces reported in the literature [7,13].

4.2.3 AT Adsorption from Plasma

ATH has been shown to inhibit coagulation via the catalytic activity of heparin by binding AT and inactivating thrombin and Factor Xa (FXa), so that FXa could not enzymatically cleave prothrombin (Factor II) to produce thrombin (Factor IIa) [29]. Therefore, the ability of a surface modified with ATH to bind AT from plasma may be used as a measure of its anticoagulant activity. Accordingly unmodified and modified PDMS surfaces were incubated in plasma containing radiolabelled AT added as a tracer. AT adsorption on unmodified PDMS was found to be $2.95 \text{ ng}/\text{cm}^2$ (Fig. 17). AT adsorption on the PEG surfaces was lower than on the unmodified PDMS ($p < 0.05$), presumably due to the intrinsic protein resistance of PEG.

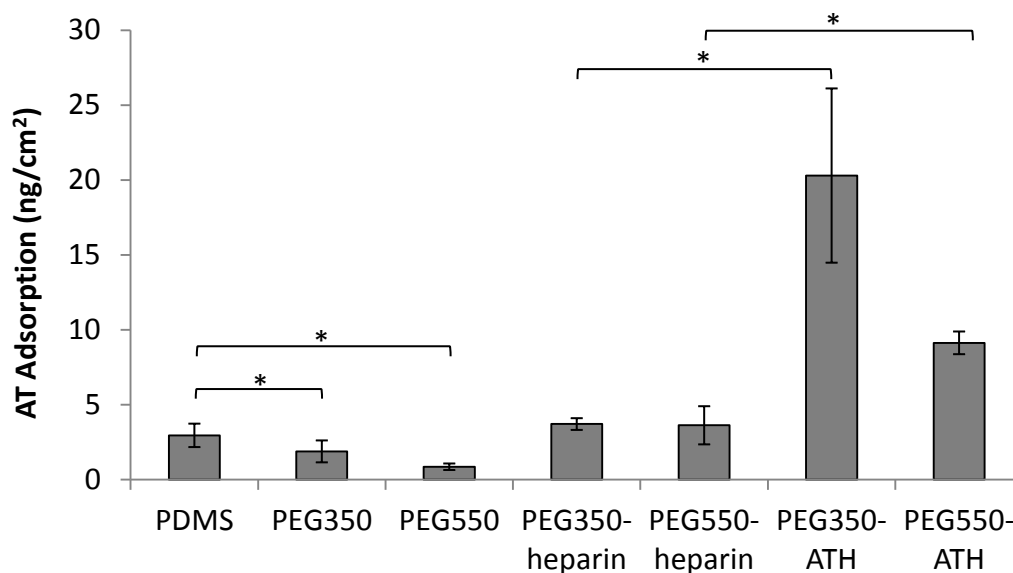


Figure 17. AT adsorption from plasma to PDMS surfaces modified with PEG, PEG-heparin and PEG-ATH. Adsorption time 3 h. Data are mean \pm SD, $n = 3$. * Significant differences ($p < 0.05$).

Since ATH is a novel anticoagulant based on heparin, it was of interest to compare the anticoagulant activity of an ATH-treated surface to an analogous surface modified with unfractionated heparin. Although UFH does bind AT in plasma, it was found that the PEG-heparin surfaces adsorbed only slightly more AT than the PEG surfaces ($p > 0.05$). However, the PEG-ATH surfaces adsorbed significantly more AT than the PEG surfaces ($p < 0.05$), as well as unmodified PDMS and the PEG-heparin surfaces ($p < 0.05$). AT adsorption was also greater on PEG350-ATH than on PEG550-ATH, likely due to the greater protein resistance of the longer PEG chains (Fig. 17).

These data demonstrate the greater ability of immobilized ATH to bind AT selectively from plasma compared to immobilized unfractionated heparin. This result is to be expected since the preparation process for ATH selects for heparin molecules having

one or more pentasaccharide AT-binding sequences. Therefore, every ATH molecule can potentially bind AT biospecifically, whereas only one-third of unfractionated heparin (UFH) has a pentasaccharide AT-binding sequence, thus limiting the ability of a heparinized surface to bind AT specifically [74].

4.2.4 Antithrombin and Fibrinogen Adsorption from the Plasma to PDMS surfaces

The purpose of the dual surface modification strategy is to inhibit non-specific protein adsorption and promote anticoagulation, so it was of interest to perform experiments to evaluate both these aspects simultaneously. Therefore, fibrinogen and AT were both radiolabelled with Na¹²⁵I and were added separately to plasma in two different 96-well plates. Surfaces were incubated in the plasma with either radiolabelled fibrinogen or AT, one set of surfaces in each plate, and fibrinogen or AT adsorption on the two sets of surfaces were measured separately.

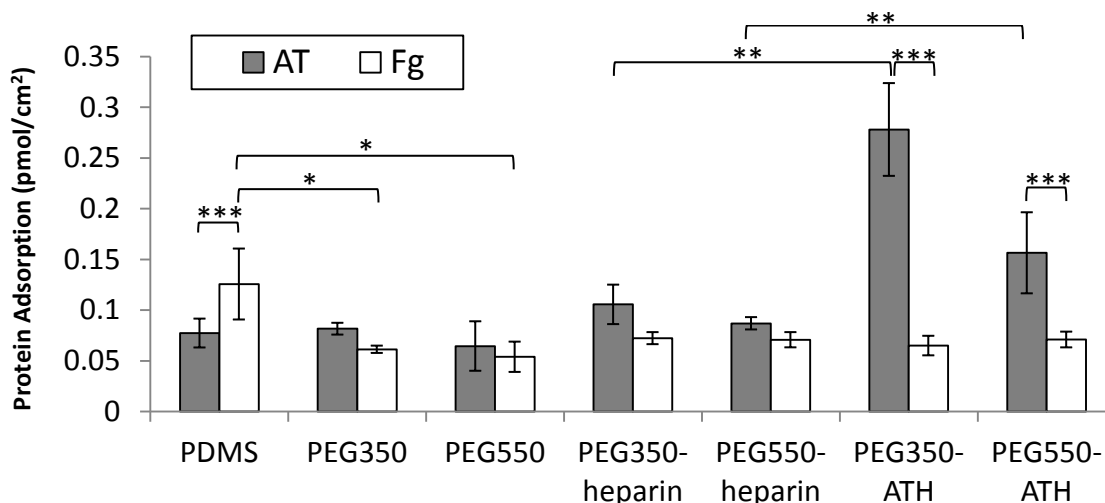


Figure 18. Antithrombin and fibrinogen adsorption from plasma to unmodified PDMS, and PDMS modified with PEG, PEG-heparin and PEG-ATH. Adsorption time 3 h. Data are mean \pm SD, n = 4. * Significant difference between surfaces in Fg adsorption ($p < 0.05$), ** significant difference between surfaces in AT adsorption ($p < 0.05$), *** significant difference between Fg and AT adsorption on the same surface ($p < 0.05$).

Fibrinogen adsorption was significantly lower on the surfaces modified with PEG in comparison to unmodified PDMS ($p < 0.05$). In addition, the quantities of fibrinogen adsorbed from plasma on PEG-ATH and PEG-heparin surfaces were similar to those on surfaces modified with PEG only, showing that conjugation of PEG with ATH or heparin did not reduce the protein resistance of the PEG chains. This may be important for inhibition of thrombosis, since adsorbed fibrinogen is a major ligand for platelet adhesion [75].

With respect to AT, the control surfaces (PDMS, PEG550, PEG350) adsorbed only small quantities. The heparin and ATH surfaces adsorbed greater quantities, but on the PEG350-ATH and PEG550-ATH surfaces adsorption was significantly greater, respectively, than on the PEG350-heparin and PEG550-heparin surfaces ($p < 0.05$), showing that the ATH-modified surfaces were more efficient at binding AT from plasma than the heparin-modified surfaces (Fig. 18), assuming that the surface densities of ATH and heparin were similar. Since heparin has been shown to bind a variety of proteins from plasma, such as vitronectin and von Willebrand factor, it may be that AT adsorption on PEG-heparin surfaces may be limited by heparin's lack of selectivity for AT in plasma, and that the anticoagulant activity of the PEG-heparin surfaces may be compromised by the non-specific binding of plasma proteins to heparin [30,31]. The PEG350-ATH surface also showed the highest AT adsorption, consistent with the data in Fig. 18. AT adsorption on PEG550-ATH was lower than on PEG350-ATH, which may be partly due to the longer PEG chains exhibiting greater resistance to protein adsorption.

Since fibrinogen and AT adsorption were measured simultaneously on two sets of surfaces, they can be compared on a molar basis to evaluate both aspects of the dual surface modification strategy. Fibrinogen adsorption was taken as a measure of non-specific protein adsorption, and AT adsorption as a measure of anticoagulant activity. On the unmodified PDMS surface, fibrinogen adsorption was significantly greater than AT on a molar basis ($p < 0.05$), presumably reflecting the higher concentration of fibrinogen in the plasma (Fig. 18). However, the PEG350-ATH and PEG550-ATH surfaces adsorbed significantly more AT than fibrinogen ($p < 0.05$) (Fig. 18). In contrast, fibrinogen adsorption was similar to AT adsorption on both of the PEG-heparin surfaces. These data illustrate the high selectivity of the PEG-ATH surfaces for AT adsorption from plasma, and suggest that they may possess some anticoagulant activity in contact with blood.

4.2.5 Adsorption of antithrombin from plasma to NaIO_4 - NaBH_4 -treated surfaces.

To investigate to what extent AT binding on the ATH- and heparin-modified surfaces was by specific interaction with the pentasaccharide sequence of heparin, PEG-heparin and PEG-ATH surfaces were treated with NaIO_4 and then with NaBH_4 to destroy the sequence [51]. As seen in Fig. 19, AT adsorption on the treated surfaces was lower than on the untreated surfaces and consistently below 3 ng/cm^2 . This quantity is comparable to AT adsorption on unmodified PDMS ($2.98 \pm 0.61 \text{ ng/cm}^2$), suggesting that the interaction of AT with the NaIO_4 - NaBH_4 -treated surfaces is likely via physical adsorption.

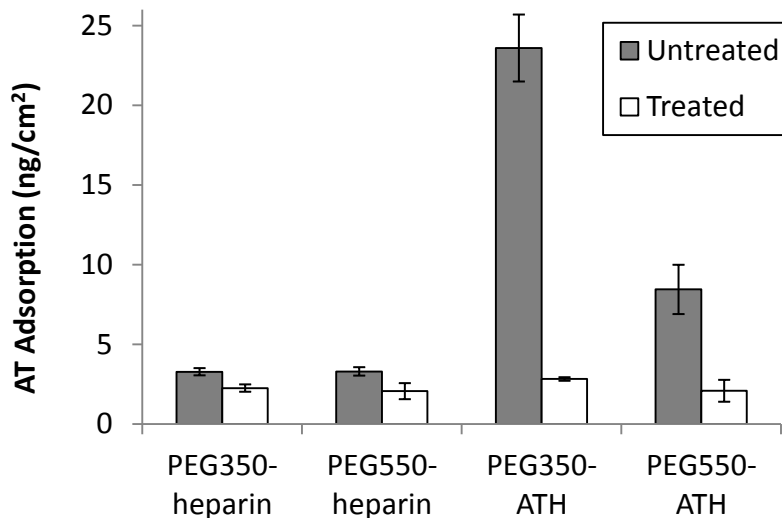


Figure 19. Antithrombin adsorption from plasma to PDMS surfaces modified with PEG and either ATH or heparin. Surfaces were treated or not treated with NaIO_4 and NaBH_4 to selectively destroy the AT-binding pentasaccharide sequence. Data are mean \pm SD, $n = 3$.

In comparison to the treated surfaces, AT adsorption on the untreated surfaces was higher for the PEG-heparin surfaces ($p > 0.05$), and significantly higher for the PEG-ATH surfaces ($p < 0.05$). These data demonstrate that AT binding to the ATH surfaces occurred by specific interaction with the pentasaccharide sequence of heparin, as expected since all heparin moieties in ATH have at least one pentasaccharide sequence, and 30-40% have two or more [35]. Consistent with data shown in Fig. 17 and 18, AT adsorption was significantly higher on PEG-ATH surfaces than on PEG-heparin surfaces, which suggests that ATH-modified surfaces may have higher anticoagulant potential than analogous heparin-modified surfaces, due to higher selectivity and specific binding of AT from plasma.

4.2.6 Western Blotting

SDS-PAGE and Western blotting were used to investigate the interactions of the surfaces with a range of plasma proteins as shown in Fig. 20. HMWK and fibronectin were not detected on any of the surfaces. In general strong bands were seen on the blots for fibrinogen, albumin, IgG, vitronectin and apolipoprotein-AI. Adsorbed fibrinogen and IgG are known to provide ligands for platelet and leukocyte adhesion, and thus may be seen as prothrombotic [76]. In general, the surfaces modified with PEG showed weaker responses (reduced adsorption) compared to the unmodified PDMS. Band intensities for the PEG surfaces were noticeably lower for fibrinogen, in agreement with the data from the radiolabelling experiments. Reductions in band intensities for albumin, IgG, vitronectin and apo-AI on the PEG surfaces were also observed.

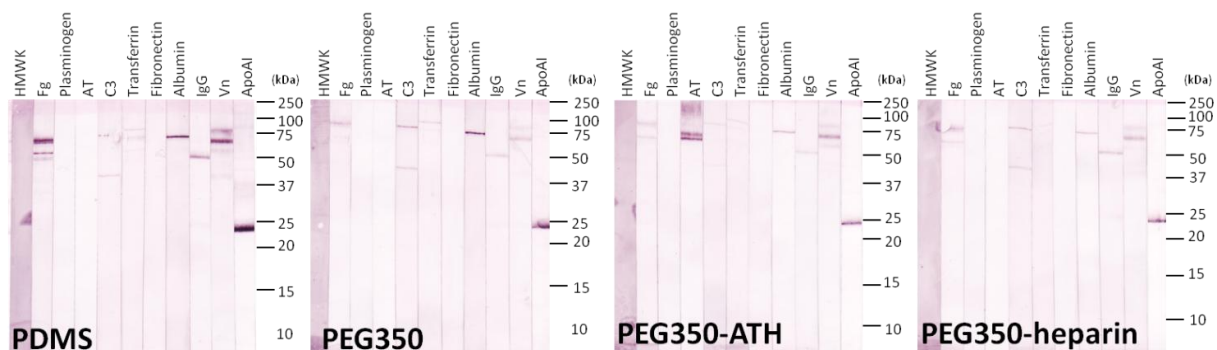


Figure 20. Western blots of proteins eluted from PDMS, PEG350, PEG350-ATH and PEG350-heparin surfaces after incubation in plasma. Blots were probed with antibodies against HMWK, fibrinogen (Fg), plasminogen, antithrombin (AT), C3, transferrin, fibronectin, albumin, immunoglobulin G (IgG), vitronectin (Vn) and apolipoprotein-AI (ApoAI).

C3 was detected on all of the surfaces as two faint bands at 75 and 40 kDa. C3 has a heavy chain at 110 kDa and a light chain at 75 kDa, and activation of the complement

system results in cleavage of C3 to give C3a and C3b [77]. The bands at 75 kDa in Fig. 20 correspond to the light chain of C3, and the bands at 40 kDa likely correspond to a fragment related to C3b [70,77]. On the basis of the C3 blots, complement activation was observed on all of the surfaces, but appeared to be the lowest on PEG350-ATH.

With the notable exception of PEG350-ATH, AT was not detected on any of the surfaces, again correlating with the radiolabelling data which showed that ATH surfaces bound significantly more AT than any of the others. The strong AT response for the PEG350-ATH surface is indeed striking, suggesting that this surface may be expected to be resistant to coagulation in contact with blood.

4.3 Thromboelastography (TEG)

The experiments discussed above were designed to investigate interactions between the PDMS surfaces and specific proteins in plasma, and the results suggested “indirectly” that the ATH-modified surfaces may have anticoagulant properties. Using TEG, the effects of the ATH-modified surfaces on coagulation were evaluated directly. Specifically the TEG response of unmodified PDMS and ATH-modified PDMS were compared.

4.3.1 TEG for PDMS modified with ATH by physical adsorption.

Typical TEG data for PDMS-ATH and unmodified PDMS are shown in Table 3. The initiation of coagulation on PDMS(ATH) was delayed compared to unmodified

PDMS as indicated by the longer reaction times (R) of 23.4 min and 16.4 min respectively, although the difference is not significant ($p>0.05$).

Table 3. TEG results for unmodified PDMS and PDMS with ATH physically adsorbed. Data are means \pm SD (n = 2). Parameters: R (reaction time), K (coagulation time), α (rate of clot development), MA (maximum amplitude).

	R (min)	K (min)	α (degrees)	MA (mm)
PDMS	16.4 \pm 1.0	4.5 \pm 0.4	34.2 \pm 3.7	26.5 \pm 0.7
PDMS(ATH)	23.4 \pm 5.4	N/A	6.3 \pm 2.1	10.9 \pm 1.6

N/A indicates that the parameter is undefined because the criterion was not met.

The coagulation time (K) was not defined for PDMS(ATH) since the curve did not reach an amplitude of 20 mm, indicating slower clot development and a weaker clot. The rate of clot development (α) and the maximum amplitude (MA) may be seen as complements to the coagulation time (K). An α -angle of 6.3° was found for PDMS(ATH), which was much lower than the 34.2° for PDMS. These data show that coagulation occurred at a much slower rate when ATH was present on the PDMS. Also the clot formed on PDMS(ATH) was mechanically weaker, as indicated by a lower maximum amplitude (MA) of 10.9 mm compared to 26.5 mm for unmodified PDMS.

Overall, comparison of these two surfaces showed that the presence of ATH on the surface of PDMS delayed the initiation of coagulation, slowed the development of the clot, and ultimately resulted in a weaker clot, all of which suggests that ATH adsorbed on PDMS gives a surface with anticoagulant properties.

Two replicate TEG experiments were performed for each surface (n=2). This small sample size was chosen since sample preparation was highly time- and resource-consuming.

The TEG results suggest that the physical adsorption of ATH on PDMS may be a simple and effective strategy for improving the blood compatibility of PDMS depending on the application. However, since the ATH is physically adsorbed it will almost certainly be removed, at least in part, from the surface during blood or plasma contact by exchange with other proteins and blood components. Data from an experiment where the surface was prepared using radiolabelled ATH showed that after 3 h incubation in plasma about 80% of the pre-adsorbed ATH remained on the surface (data not shown). Since the duration of a TEG run was usually below 1 h, ATH desorption was not significant, and the low levels of ATH generated in the plasma by desorption were unlikely to produce an anticoagulant effect. A separate TEG experiment was conducted to show that the amount of ATH that may have desorbed from the surface of PDMS(ATH) did not contribute significantly to the delay in coagulation shown on PDMS(ATH) surfaces, and that the anticoagulant effect of the PDMS(ATH) surfaces was predominantly due to the adsorbed ATH, not to ATH in solution due to desorption.

These experiments showed that TEG is a suitable technique for evaluating the effects of biomaterials on the coagulation process. TEG provided information on clot initiation, clot development and clot strength, which was useful in evaluating the effects of ATH-modification on anticoagulant properties.

4.3.2 TEG experiments on PDMS modified with covalently bound ATH via PEG spacer.

Surface preparation for these experiments was more complicated than for the physical adsorption case. As indicated previously the PDMS coating on the TEG cups had to be exposed for several hours to various solvents during surface modification and therefore it had to be relatively thick initially (at least 0.5 mm) to remain intact. The thicker PDMS coating on the cup interfered with the determination of the TEG parameters (R-time, K-time, α -angle, MA). At the beginning of the experiment when the cup was oscillated, resistance was detected since the TEG pin came in contact with the cup, causing divergence of the curves at the very beginning of the run (Fig. 21). Normally resistance is not detected until fibrin formation occurs at the initiation of clotting, generally several minutes after the run begins. The instrument determines the reaction time (R) as the time when the curves diverge with an amplitude of 2 mm. Resistance due to the PDMS coating interfered with this calculation; the other TEG parameters (K-time, α -angle, MA), several of which depend on R, were also in error. The data generated by the instrument were therefore invalid and had to be discarded.

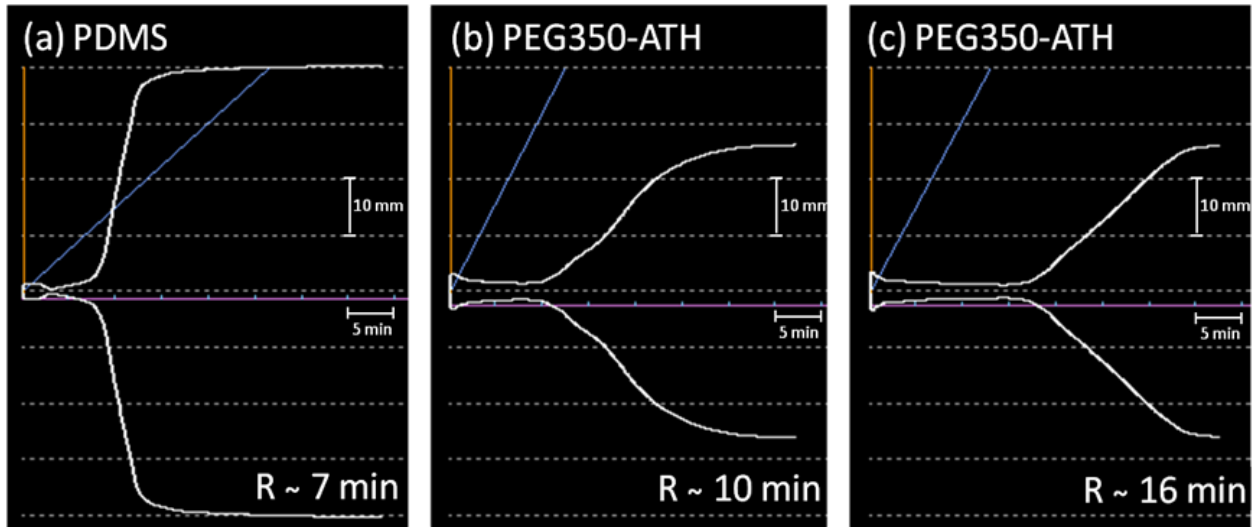


Figure 21. TEG data shown in graphical form. Three separate runs are shown with: (a) PDMS, (b) PEG350-ATH, (c) PEG350-ATH. A single PDMS and two PEG350-ATH surfaces were tested. X-axis is time (min), y-axis is distance. The reaction time (R) was estimated from each graph.

The data in Fig. 21 were analyzed manually/qualitatively. In general, the coagulation profiles for the PEG350-ATH surface (Fig. 21b and c) were less steep than that of the unmodified PDMS (Fig. 21a), indicating a lower rate of clot development on the ATH-modified surface. The initiation of coagulation was delayed as indicated by the R values: 7 min for PDMS compared to 10 and 16 min, respectively, for the two PEG350-ATH surfaces. Since clot development was slower on the ATH-modified surfaces, the resulting clots were weaker, as indicated by the smaller amplitudes. Thus PDMS surfaces modified with ATH and with PEG350 as a spacer delayed the initiation of coagulation, prolonged clot formation, and the resulting clot was weaker compared to unmodified PDMS.

The experiments in this work showed that the TEG method may be feasible as a means of evaluating the coagulant effects of some surfaces, and produced some

preliminary data, thus providing the basis for future experiments with larger sample sizes to give more reliable results. The procedure for coating the TEG cups with PDMS needs to be modified to ensure that the PDMS coating does not interfere with the analysis. The cup inner diameter should be reduced to allow for the thick PDMS coating. The goal would be to keep the inner diameter, and therefore the volume, of the coated cup roughly the same as that of the uncoated cup; this should overcome the problem of contact between the cup and the pin during operation. The TEG method is intrinsically sensitive, straightforward, and reproducible, providing important information on coagulation, in the form of parameters that can be easily analyzed. Therefore if sample preparation problems can be overcome, it should prove to be a valuable method for evaluation of blood contacting biomaterials.

The use of TEG to evaluate the thrombogenicity of biomaterials has been reported in literature. Two methods have been used for TEG analysis of biomaterial effects. In the first method, the biomaterial is incubated in blood, and the resulting blood is subjected to TEG analysis; examples of biomaterials analyzed include glass, cellulose, Tygon, and a heparin-coated catheter [65,78,79]. Many studies have used this method to avoid the surface preparation necessary to analyze materials directly by TEG; a disadvantage is that the blood is not in direct contact with the biomaterial during analysis. In the second method, polymeric biomaterials are used in microparticle form and are added to the blood for TEG analysis. For example, ceramic biomaterials such as silicon carbide and bioactive glass, were ground to a fine powder for TEG analysis [64]. It was found that the usable amount of powder was limited (~20 mg), since excessive powder in the cup

could interfere with its motion [64]. In this work, PDMS was dip-coated onto the TEG cup, resulting in the PDMS film being in direct contact with the plasma during TEG analysis, thus resembling more closely in vivo conditions of blood flow across the surface of the biomaterial.

The use of TEG for the evaluation of the surface modification strategy in the present study was unique in several aspects. The anticoagulant potential of biomaterials modified with ATH have been evaluated in previous investigations with a clotting assay based on absorbance measurements, and in rabbit models using endoluminal grafts and catheters, but the use of TEG to evaluate PDMS modified with PEG-ATH is unique in this work [48,50–52]. The PEG and ATH modified surfaces were relatively complex compared to other surfaces evaluated with TEG as reported in the literature. These include surfaces coated with heparin or endothelial cells by physical adsorption [64,65]. In the present work new methods for the study of blood-material interactions with TEG have been developed, and the feasibility of TEG as a method for the evaluation of PDMS modified with PEG and ATH has been demonstrated.

5. DEVELOPMENT OF BLOOD OXYGENATOR FOR NEONATES.

5.1 Introduction

This chapter describes work done on the development of a microfluidic blood oxygenator as a lung assist device for preterm infants. The work was in collaboration with the labs of Drs. C. Fusch and P. Selvaganapathy. These labs have developed the concept of an artificial placenta involving a microfluidic extracorporeal membrane oxygenator connected to the infant via the umbilical vessels (Fig. 23). It was developed for the use of premature infants (22-36 weeks gestation) suffering from respiratory distress requiring support [80]. The work in our lab involved adaptation of the procedures developed for the modification of PDMS with ATH to the PDMS surfaces of the oxygenator device.

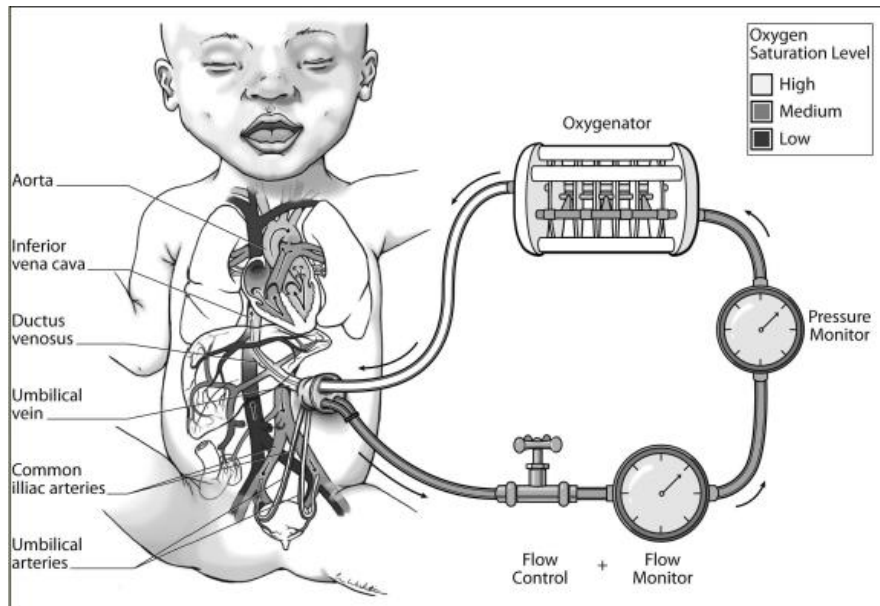


Figure 22. Circulation of blood from the infant to the oxygenator via the umbilical vessels (from <http://bmc.erin.utoronto.ca/~erinw/d3.html>).

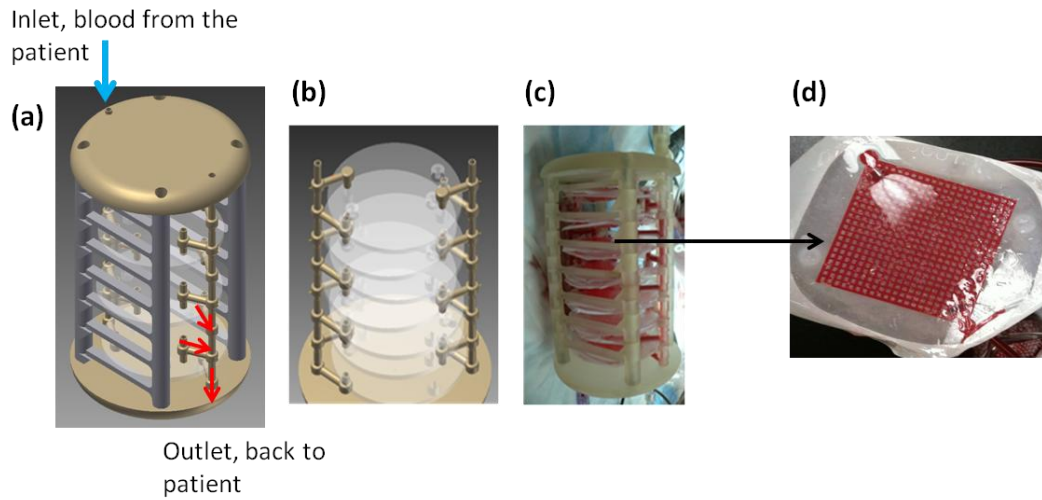


Figure 23. Different views of the oxygenator: (a) Schematic showing 14 modules stacked up in the oxygenator, direction of blood flow also indicated by arrows (b) View of (a) without the skeleton structure, the 14 modules are connected in parallel (c) photograph of oxygenator with blood flow (d) single oxygenator module. (Adapted from [81]).

The oxygenator consists of fourteen modules stacked symmetrically in parallel (Fig. 23), with blood flow uniformly distributed in each module [81]. The modules consist of a microfluidic network made from PDMS and polycarbonate. Oxygen and blood flow on opposite sides of the gas-permeable PDMS/polycarbonate microchannels. A single module is shown in Fig. 23d and 24a, indicating the network (grid) of microfluidic channels. Fig. 24b shows a schematic view of the channel grid. Venous blood enters at the inlet, travels through the channels where gas exchange takes place, and leaves through the outlet as oxygenated blood [80]. Fig. 24c shows a side view of the oxygenator. The gas exchange membrane allows for the exchange of O_2 and CO_2 , and the microfluidic network provides a high surface to volume ratio to give gas exchange with sufficient throughput [80].

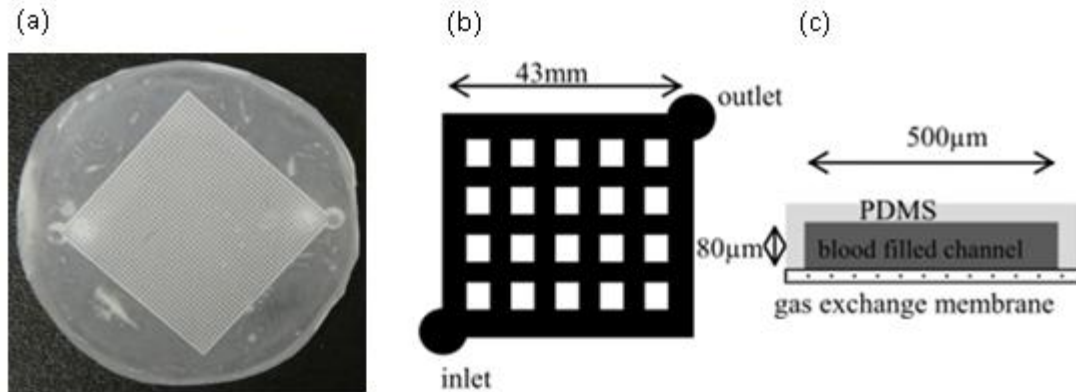


Figure 24. Single oxygenator module: (a) photograph, top view of module, (b) schematic of microfluidic network, (c) side view (Adapted from [80]).

The design of the oxygenator is complex and encompasses many aspects. The blood must distribute uniformly among the channels as it flows through the device, the hydraulic resistance must be minimal, and a sufficient number of modules must be assembled for the required rates of gas exchange [80]. An important aspect of the design is biocompatibility: the oxygenator may be required to function for several days and surface-activated thrombosis must be prevented. Not only is thrombosis life-threatening to the patient, but the formation of blood clots within the oxygenator blocks the flow in the microchannels, compromising gas transfer and eventually leading to device failure.

Modification of the surfaces of the oxygenator with an anticoagulant such as ATH may help to prevent thrombosis due to blood-material contact and thus improve the blood compatibility of the device.

In initial work the oxygenator surfaces were coated with ATH by physical adsorption, a very simple method with no need for chemical modification. Experiments of three types were conducted to evaluate the feasibility of this approach. In type 1, human

serum albumin (a cheap alternative to ATH for preliminary work) was adsorbed from solution to the oxygenator microchannels which were then exposed to flowing buffer solution to determine the durability of the adsorbed layer. Protein on the surface was monitored by gold staining. Type 2 was the same as type 1 except that adsorption/desorption was monitored by measuring HSA concentration in solution. In type 3, ATH was used and 6 mm diameter discs of PDMS cut from films were used in place of the oxygenator modules. Adsorption was from buffer and was followed by incubation in whole blood under static conditions over 3 days. The quantity of protein on the surface was determined.

5.2 Materials and Methods

5.2.1 HSA adsorption on oxygenators: visualization with gold stain.

Six oxygenator modules were connected in series and PBS was circulated for 15 min, followed by 10 mL of HSA (0.1 mg/mL in PBS, 5% radiolabelled) for 3 h. The flow rate was maintained at 5 mL/min, and when a module developed a leak, it was removed from the circuit to prevent loss of re-circulating fluid. The flow rate was reduced accordingly. After 3 h the HSA was drained and unbound protein was washed out of the circuit with PBS (three times 5 min each time).

For protein visualization a solution of gold stain (BB International, Cardiff, UK) was circulated for 2 h, drained and the circuit rinsed with water three times (5 min each time).

5.2.2 HSA adsorption on oxygenators followed by incubation in buffer and determination of protein concentration.

Two separate circuits (A and B) were used with three oxygenator modules connected in series. PBS was circulated for 15 min, and HSA solution (0.1 mg/mL in PBS, 5% radiolabelled) was then added. After 2 h the HSA was drained from the circuits. The flow rate for all steps was 1 mL/min.

For circuit A, the system was rinsed with PBS (three times, 5 min each time). All rinse liquids were collected. The grid portions of the modules were cut into 3 sections, inlet, centre, and outlet according to Fig. 25a, and the associated radioactivity was determined. The counts for the 3 sections were combined to determine the quantity of HSA adsorbed to the oxygenator surfaces. After this initial analysis, the three sections were punched into discs (Fig. 25b) and the radioactivity determined again to evaluate the distribution of adsorbed HSA in the oxygenator.

For circuit B, PBS was added and circulated for 1 h before drainage. Radioactivity was determined as described for circuit A.

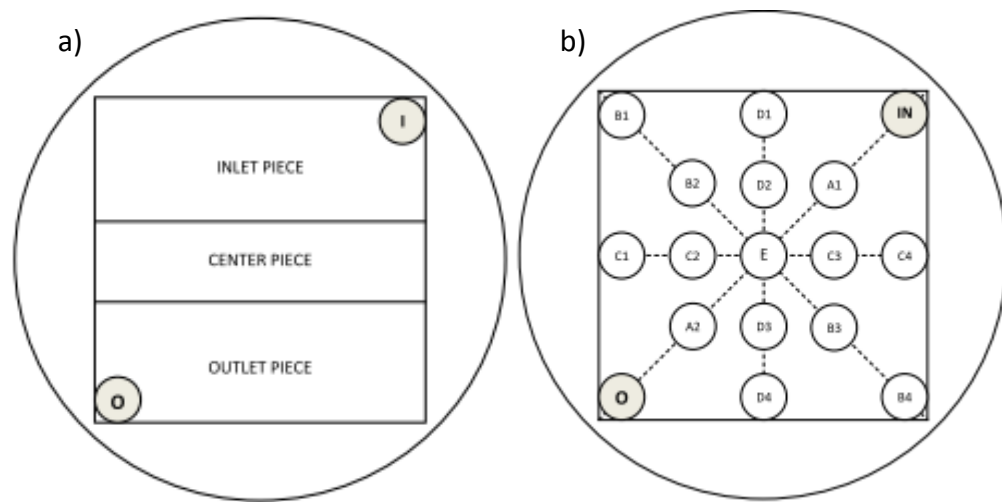


Figure 25. Schematics (a&b) of oxygenator divided into sections for analysis.

5.2.3 ATH adsorption on PDMS discs followed by incubation in blood.

PDMS films were punched into 6 mm diameter discs, which were incubated in ATH solution (0.1 mg/mL in PBS, 10% radiolabelled) in 96-well plates. Surfaces were rinsed three times with PBS, 5 min each time. The discs were then transferred to 48-well plates with 2 mL of whole blood (McMaster Hospital Blood Bank, Hamilton, ON) in each well, and incubated for varying times, rinsed three times in PBS, 5 min each time, and radioactivity determined. The 48-well plates were placed on a shaker during incubation to keep the blood well mixed. The blood was replaced every 24 h to avoid settling of cells and bacterial growth.

5.3 Results and Discussion

5.3.1 HSA adsorption on oxygenators: visualization with gold stain.

The microchannels of the oxygenators were contacted with HSA by the continuous flow of the protein solution in the circuit. Gold staining of the modules after HSA contact confirmed that the protein was adsorbed to the microchannels, but the distribution was not uniform in the grid as indicated by the darker and lighter patches (Fig. 26).

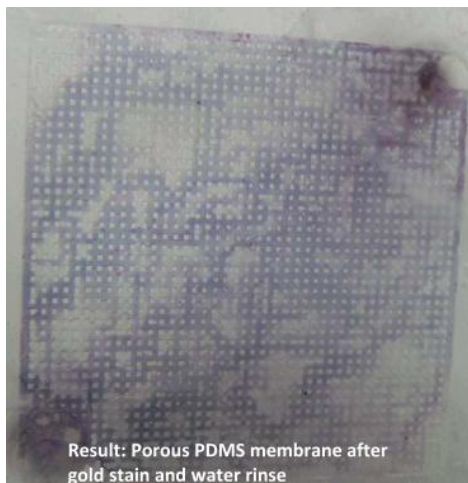


Figure 26. Grid of micro-channels in oxygenator module after HSA adsorption and gold staining. Purple colour indicates protein adsorbed on the inside surface of the microchannels.

Several problems related to flow were encountered during these experiments. First, leakage occurred due to poor assembly of the devices. Therefore it was important for each oxygenator to undergo leakage tests using relatively high flow rates for at least an hour prior to experiments. Second, flow was not evenly distributed throughout the grid. Increasing the flow rate improved the distribution, but there were still stagnant regions, and liquid travelled directly from the inlet to the outlet through only a few “channels” leaving much of the grid surface unused. Also over the course of the experiment, it was obvious that some of the microchannels were blocked by air bubbles (Fig. 27).



Figure 27. Microchannel grid showing regions blocked by air bubbles when PBS was circulated.

Although the channel surfaces could be coated by physical adsorption of a protein by circulating protein solution at low flow rate, the design and the process need to be improved to ensure even flow distribution in the grid, so that all surfaces are exposed to blood during oxygenation. Possibilities to prevent the blockage of microchannels by air bubbles, are to degas the fluids to remove dissolved gases, and to circulate the fluids under vacuum to reduce the pressure at the outlet and help to “pull” the liquid through the circuit.

5.3.2 HSA adsorption to oxygenators followed by incubation in buffer and determination of residual protein by concentration measurements.

The stability of the adsorbed HSA layer in the oxygenators was evaluated by incubating with PBS for 1 h. Table 4 shows HSA adsorption levels averaged over the entire surface area of a module before and after incubation with PBS. The values, $0.17 \mu\text{g}/\text{cm}^2$ and $0.13 \mu\text{g}/\text{cm}^2$, respectively, were not significantly different indicating that the adsorbed HSA layer was not significantly eluted by PBS, and therefore could be seen as relatively stable on the PDMS surface.

Table 4. HSA adsorption on grid before and after incubation with PBS.

	HSA adsorbed on grid ($\mu\text{g}/\text{cm}^2$)
Before PBS	0.17
After PBS	0.13

Table 5. HSA adsorption on sections of grid before and after incubation with PBS (see Fig. 26b for nomenclature of grid sections).

	Before PBS	After PBS
Grid section	HSA adsorbed ($\mu\text{g}/\text{cm}^2$)	HSA adsorbed ($\mu\text{g}/\text{cm}^2$)
A1	0.43	0.30
A2	0.33	0.59
B1	0.47	0.54
B2	0.41	0.50
B3	0.28	0.46
B4	0.30	0.41
C1	0.40	0.76
C2	0.39	0.56
C3	0.39	0.43

	Before PBS	After PBS
Grid section	HSA adsorbed ($\mu\text{g}/\text{cm}^2$)	HSA adsorbed ($\mu\text{g}/\text{cm}^2$)
C4	0.36	0.39
D1	0.50	0.40
D2	0.47	0.39
D3	0.45	0.55
D4	0.33	0.77
E	0.36	0.51
AVERAGE	0.39	0.50
MIN	0.28	0.30
MAX	0.50	0.77

A similar analysis was done using small areas of the grid to evaluate adsorption and desorption in different regions. Similar to the overall data in table 4, incubation with PBS did not cause significant desorption of HSA from any specific region of the grid (Table 5). The HSA adsorption levels in table 5 were in general higher than those in table 4, possibly due to uncertainties in determining the surface area of the microchannels.

5.3.3 ATH adsorption on PDMS discs followed by incubation in blood.

In these experiments PDMS discs were coated with ATH by physical adsorption, and were then incubated in blood. This protocol was expected to provide a more severe test of the stability of adsorbed protein layers on PDMS. The data in Fig. 28 show that the adsorbed ATH desorbed slowly from the surfaces over a 3-day period. The starting adsorption level of ATH was $0.18 \mu\text{g}/\text{cm}^2$, close to the estimated monolayer quantity of $0.23 \mu\text{g}/\text{cm}^2$ [13]. After 1 h of incubation in blood, only 62% ($0.11 \mu\text{g}/\text{cm}^2$) remained, and after 3 h, only 48% remained. Thus ATH desorption occurred more rapidly in blood than in buffer (Tables 4 and 5), likely due to exchange with other plasma proteins [82]. It should also be noted that the blood data (Fig. 28) were obtained under static conditions; the presence of fluid shear flow would probably increase the rate of desorption further.

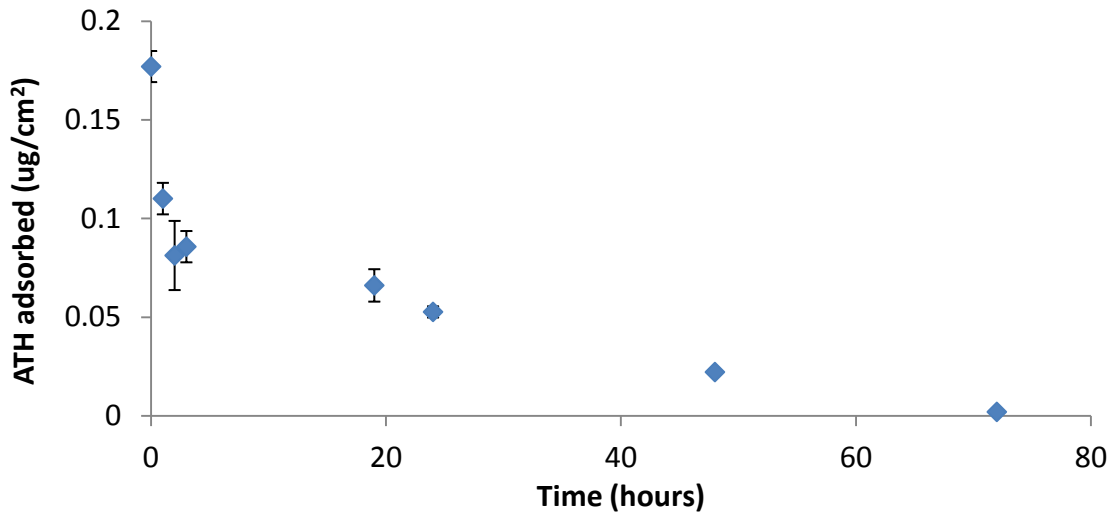


Figure 28. Desorption of ATH from PDMS discs in contact with blood. Data are mean \pm SD, $n = 3$.

The microfluidic oxygenator was designed to provide respiratory support to preterm infants over periods on the order of several days. The data in Fig. 28 indicate that over half of the physically adsorbed ATH was desorbed from the PDMS surface in 3 h, leaving bare PDMS in direct contact with blood to provoke adverse blood-material interactions leading to coagulation and thrombosis. After 3 days, ~99% of the ATH was desorbed, indicating that the ATH coating was essentially removed on exposure to blood. It thus appears that physical adsorption is not feasible as a method for modification of PDMS surface with ATH.

5.3.4 Discussion and Conclusions

Initial experiments showed that coating the surfaces of the oxygenator with HSA by physical adsorption gave surface coverage close to monolayer values. During the coating process, it is important that all the surfaces in the oxygenator be evenly coated. Blockage of microchannels by air bubbles, leading to uncoated areas, was observed and it

is suggested that this may be mitigated by degassing the protein solution and applying negative pressure at the device exit.

In general, the radiolabelling and gold staining data showed that the HSA layer was stable in contact with PBS. However, when PDMS was coated with ATH by physical adsorption and exposed to blood, over half of the ATH was desorbed after 3 hours, and almost no ATH remained on the surface after 3 days. The adsorbed ATH was likely exchanged with other proteins in blood. It is concluded, therefore, that modification with ATH by physical adsorption is not feasible given that oxygenators must remain functional in contact with flowing blood for several days.

A more stable surface coating may be achieved by covalent immobilization of ATH via a PEG spacer. However, since the geometry of the microchannel grid is complex, the surface modification procedure should preferably be simple. The chemical reactions involved in covalent immobilization, requiring the circulation of solvents and reagents over periods of several hours may not be suitable.

In continuing experimental work on this project the use of polydopamine as a “bioglue” to attach ATH to PDMS is being explored. Polydopamine, a mussel-inspired adhesive, is gaining recognition as a highly effective, simple approach for attaching biomolecules to surfaces [83,84]. No complicated chemical reactions are involved, only a 2-step solution coating procedure. It is hoped that polydopamine will retain ATH at the PDMS surface more effectively than physical adsorption. In work so far polydopamine/ATH layers have been shown to be stable when exposed to plasma and even to SDS.

6. SUMMARY AND RECOMMENDATIONS FOR FURTHER WORK

6.1 Summary

To combat the predisposition of blood-contacting PDMS to cause thrombosis, ATH was grafted to PDMS using as a PEG spacer/linker. This dual surface modification strategy was designed to provide both resistance to non-specific protein adsorption (PEG) and anticoagulant activity.

Surface modification with PEG was confirmed by water contact angle measurements and XPS: the advancing contact angle of the PDMS surface was reduced from $>100^\circ$ to about 70° , and the carbon and oxygen contents increased after modification with PEG. Using NHS chemistry ATH was attached covalently to the distal chain end of the PEG; attachment was confirmed by an increase in nitrogen content as determined by XPS. The surface concentration of ATH on the PEG350-NHS and PEG550-NHS surfaces was determined to be $0.16 \mu\text{g}/\text{cm}^2$ and $0.09 \mu\text{g}/\text{cm}^2$, respectively, after treating with SDS, representing the amount of ATH that was strongly (presumably covalently) bound to the PDMS surface.

From investigation of the interactions of plasma proteins with the PDMS surfaces it was shown that, in general, modification with PEG effectively reduced non-specific protein adsorption, and that immobilization of ATH at the distal end of the PEG chains did not significantly affect protein resistance. Fibrinogen adsorption from buffer was reduced by $>90\%$ on the PEG550-grafted surface compared to the unmodified PDMS. Western blot analysis showed that surfaces modified with PEG resisted the adsorption of a range of plasma proteins including albumin, fibrinogen, IgG and apolipoprotein-AI.

Since ATH was developed to overcome the limitations of heparin, it was of interest to compare the performance of an ATH-modified surface with that of an analogous heparin-modified surface. Because ATH and heparin have the ability to inhibit coagulation catalytically by binding AT in blood, AT adsorption on these surfaces was measured as an indication of anticoagulant potential. Radiolabelling and Western blot data showed that the ATH-modified surfaces bound significantly more AT from plasma than unmodified PDMS, PDMS-PEG and PDMS-PEG-heparin surfaces. AT uptake on the ATH-modified surfaces was shown to be specific through the pentasaccharide sequence on the heparin moiety of ATH. Therefore, assuming that the surface density of heparin was similar to that of ATH on a molar basis, the ATH-modified surfaces showed higher efficiency for AT binding than the heparin-modified ones, given that the modification reactions used to covalently attach heparin were analogous to those for ATH. Surfaces modified with ATH were found to have greater anticoagulant activity than those modified with heparin. The superior properties of the ATH surfaces are likely due to the fact that every ATH molecule has at least one pentasaccharide sequence, compared to only one third for the UFH molecules.

Thromboelastography (TEG) was used to further investigate the anticoagulant properties of the ATH-modified surfaces by measuring the effect of these surfaces on the coagulation process directly. The TEG experiments indicated a delay in the initiation of coagulation on the ATH-modified surfaces compared to the unmodified PDMS. Also on the ATH-modified surfaces, coagulation was slower, and the resulting clots were weaker in comparison to PDMS. Coagulation was delayed and prolonged on PDMS modified

with ATH via a PEG spacer. The TEG results are considered to be qualitative and preliminary.

6.2 Recommendations for Future Work

6.2.1 Surface Modification with PEG and ATH

In this project, the use of a dual surface modification strategy to improve the blood compatibility of PDMS was investigated. The two elements of the strategy are inhibition of non-specific protein adsorption and promotion of anticoagulant activity. The surface modification procedure consists of a series of chemical reactions, where the modification in each step is limited by the preceding one; therefore the outcome of surface modification could vary. First the surface of PDMS was functionalized with SiH groups, followed by PEG attachment via hydrosilylation. Modification with SiH groups and PEG was confirmed by XPS and contact angle measurements. However, the surface densities of SiH groups and PEG could not be directly quantified in this work, and the efficiency of each modification step was difficult to determine. As a result determination of reaction conditions to maximize the surface density of PEG was problematic. This is important because the surface density of ATH/heparin is dependent on the PEG density. In future investigations, alternative methods of modifying PDMS with PEG should be studied to find an efficient and reproducible one. For example instead of modifying the surface of PDMS, polyhydromethylsiloxane could be crosslinked and prepared in film form by the sol-gel process, resulting in SiH groups in bulk and on the surface of the film

for further modification [85,86]. Alternatively, block copolymers that incorporate PDMS and PEG blocks could be used [87].

In this work, PEG of two different molecular weights (350 and 550 Da) was used. Higher molecular weights, above 1000, should also be investigated since PEG molecular weight is known to influence protein resistance, with longer chains giving greater resistance [73]. Other than chain length, resistance to non-specific protein adsorption is also dependent on the density of the PEG. Because the PEG density could not be determined, the PDMS-PEG surfaces were evaluated based on the inhibition of non-specific protein adsorption using radiolabelling and Western blotting. A method to quantify the amount of PEG on PDMS would be helpful to optimize reaction conditions and to determine the optimal PEG chain length for protein resistance.

The second aspect of the dual surface modification strategy is the immobilization of heparin/ATH to promote anticoagulation. The surface density of ATH was determined by radiolabelling experiments, but this technique is not suitable for heparin. Modification with heparin was indirectly confirmed by the adsorption of AT from buffer and plasma. XPS was used to detect heparin based on sulfur content on the PDMS-PEG550-heparin surface, but only trace amounts were found. Additional XPS analyses should be done on the PDMS-PEG350-heparin surface expected to have a higher heparin density. The use of a toluidine blue assay has been reported in the literature for measuring heparin density on surfaces, but it is likely that the heparin content of surfaces in this work may be below the detection limit of this assay [88,89]. A surface-sensitive method is needed to determine

the density of heparin on the modified surfaces for a better comparison of bioactivity with other surfaces.

In future work, the optimal balance between the two aspects of the dual surface modification strategy should be investigated in detail. Since ATH was conjugated to the distal end of the PEG chains, the density of covalently bound ATH was limited by the density of PEG chains. In addition, the protein-repellent nature of PEG may reduce the amount of ATH uptake on the surface. Factors such as PEG chain length, PEG density and ATH density have to be taken into consideration for optimization of the surface in terms of inhibition of non-specific protein adsorption and promotion of anticoagulant activity.

6.2.2 Interactions with other proteins and blood components

In this project, AT adsorption on the modified surfaces was taken as an indirect measure of anticoagulant activity. To provide additional information on the anticoagulant potential of the ATH-modified surfaces in comparison to heparin-modified surfaces, the inhibition of thrombin and FXa should also be investigated. Unlike heparin, ATH can inhibit thrombin directly through its AT component and this function could be evaluated using radiolabelling experiments.

Future experiments should be extended to investigate the interactions between ATH- and heparin-modified surfaces and other blood components such as platelets and leukocytes. This is relevant since some heparinized surfaces reported in the literature have been shown to reduce platelet and leukocyte activation, which is important for blood

compatibility [11,90]. Several techniques (SEM, radiolabelling) are available to measure platelet adhesion and activation [21,70]. Leukocyte activation can be studied by monitoring activation markers or release of granule contents [11,90].

6.2.3 Thromboelastography (TEG)

In this work, TEG was used to assess the effect of PDMS and PEG350-ATH on plasma coagulation. The preliminary data generated provide the basis for future experiments with larger sample sizes. TEG research should also be expanded to include surfaces such as PDMS, PEG350, PEG350-ATH, PEG350-heparin, PEG550, PEG550-ATH, and PEG550-heparin. The data from such experiments would potentially illustrate the effectiveness of the dual surface modification strategy for the prevention of thrombosis on PDMS. In addition, TEG could be used for experiments with whole blood to incorporate the cellular components of blood in the evaluation of thrombogenicity.

REFERENCES

1. Brash JL. Exploiting the current paradigm of blood-material interactions for the rational design of blood-compatible materials. *J Biomater Sci Polym Ed* **2000**; 11: 1135–46.
2. Pinto S, Alves P, Matos CM, Santos AC, Rodrigues LR, Teixeira JA, Gil MH. Colloids and Surfaces B: Biointerfaces Poly (dimethyl siloxane) surface modification by low pressure plasma to improve its characteristics towards biomedical applications. *Colloids Surf B Biointerfaces* **2010**; 81: 20–6.
3. Brash JL. Hydrophobic Polymer Surfaces and Their Interactions With Blood. *Ann N Y Acad Sci* **1977**; 283: 356–71.
4. Chen H, Chen Y, Sheardown H, Brook MA. Immobilization of heparin on a silicone surface through a heterobifunctional PEG spacer. *Biomaterials* **2005**; 26: 7418–24.
5. Chen H, Brook MA, Sheardown H. Silicone elastomers for reduced protein adsorption. *Biomaterials* **2004**; 25: 2273–82.
6. Abbasi F, Mirzadeh H, Katbab A-A. Modification of polysiloxane polymers for biomedical applications: a review. *Polym Int* **2001**; 50: 1279–87.
7. Mikhail AS, Ranger JJ, Liu L, Longenecker R. Rapid and Efficient Assembly of Functional Silicone Surfaces Protected by PEG : Cell Adhesion to Peptide-Modified PDMS. *J Biomater Sci Polym Ed* **2010**; 21: 821–42.
8. Farrell M, Beaudoin S. Colloids and Surfaces B : Biointerfaces Surface forces and protein adsorption on dextran- and polyethylene glycol-modified polydimethylsiloxane. *Colloids Surf B Biointerfaces* **2010**; 81: 468–75.
9. Zhou J, Yan H, Ren K, Dai W, Wu H. Convenient Method for Modifying Poly (dimethylsiloxane) with Poly (ethylene glycol) in Microfluidics. *Anal Chem* **2009**; 81: 6627–32.
10. Gorbet MB, Sefton M V. Biomaterial-associated thrombosis: roles of coagulation factors, complement, platelets and leukocytes. *Biomaterials* **2004**; 25: 5681–703.
11. Olsson P, Sanchez J, Mollnes TE. On the blood compatibility of end-point immobilized heparin. *J Biomater Sci Polym Ed* **2000**; 11: 1261–73.
12. Rezaie AR. Tryptophan 60-D in the B-Insertion Loop of Thrombin Modulates the Thrombin-Antithrombin Reaction. *Biochemistry* **1996**; 35: 1918–24.

13. Sask KN, Zhitomirsky I, Berry L, Chan A, Brash JL. Surface modification with an antithrombin-heparin complex for anticoagulation: studies on a model surface with gold as substrate. *Acta Biomater* **2010**; 6: 2911–9.
14. Chan A, Berry L, Brodovich HO, Klement P, Mitchell L, Baranowski B, Monagle P, Andrew M. Covalent Antithrombin-Heparin Complexes with High. *J Biol Chem* **1997**; 272: 22111–7.
15. Ratner BD. Biomaterials Science: an introduction to materials in medicine. 2nd ed. Ratner BD, Hoffman AS, Schoen FJ, Lemons JE, editors. San Diego, California: Elsevier Inc.; **2004**.
16. Williams DF. On the mechanisms of biocompatibility. *Biomaterials* **2008**; 29: 2941–53.
17. Courtney JM, Forbes CD. Thrombosis on foreign surfaces. *Br Med Bull* **1994**; 50: 966–81.
18. Rubens FD. Perspective Cardiopulmonary bypass technology transfer: musings of a cardiac surgeon. *J Biomater Sci Polym Ed* **2002**; 13: 485–99.
19. Courtney JM, Lamba NM, Sundaram S, Forbes CD. Biomaterials for blood-contacting applications. *Biomaterials* **1994**; 15: 737–44.
20. Andrade JD. Surface and Interfacial Aspects of Biomedical Polymers. Second Edi. Andrade JD, editor. New York, USA: Plenum Press; **1985**.
21. Tsai W, Grunkemeier JM, Mcfarland CD, Horbett TA. Platelet adhesion to polystyrene-based surfaces preadsorbed with plasmas selectively depleted in fibrinogen, fibronectin, vitronectin, or von Willebrand's factor. *J Biomed Mater Res* **2001**; 1: 4–6.
22. Brash JL, Horbett TA. Proteins at Interfaces: Physicochemical and Biochemical Studies. Washington, DC: American Chemical Society; **1987**.
23. Vroman L. When Blood Is Touched. *Materials* **2009**; 2: 1547–57.
24. Chen H, Zhang Z, Chen Y, Brook MA, Sheardown H. Protein repellent silicone surfaces by covalent immobilization of poly(ethylene oxide). *Biomaterials* **2005**; 26: 2391–9.
25. Chen H, Yuan L, Song W, Wu Z, Li D. Biocompatible polymer materials: Role of protein–surface interactions. *Prog Polym Sci* **2008**; 33: 1059–87.

26. Alibeik S, Zhu S, Brash JL. Surface modification with PEG and hirudin for protein resistance and thrombin neutralization in blood contact. *Colloids Surf B Biointerfaces* **2010**; 81: 389–96.
27. Li D, Chen H, Brash JL. Mimicking the fibrinolytic system on material surfaces. *Colloids Surf B Biointerfaces* **2011**; 86: 1–6.
28. Zwaal RFA, Hemker HC, editors. Blood Coagulation. New York, USA: Elsevier B.V.; **1986**.
29. Berry L, Becker DL, Chan A. Inhibition of fibrin-bound thrombin by a covalent antithrombin-heparin complex. *J Biochem* **2002**; 132: 167–76.
30. Berry L, Chan A. Improving Blood Compatibility. In: Chu P, Liu X, editors. *Biomaterials Fabrication and Processing Handbook* Boca Baton, Florida: CRC Press; **2007**. p. 535–73.
31. Bick RL, Frenkel EP, Walenga J, Fareed J, Hoppensteadt D a. Unfractionated heparin, low molecular weight heparins, and pentasaccharide: basic mechanism of actions, pharmacology, and clinical use. *Hematol Oncol Clin North Am* **2005**; 19: 1–51.
32. Kakkar VV, Thomas DP, editors. Heparin, Chemistry and Clinical Usage. London: Academic Press; **1976**.
33. Conrad E. Heparin-Binding Proteins. San Diego, California: Academic Press; **1998**.
34. Weitz J. Low-molecular-weight heparins. *N Engl J Med* **1997**; 337: 688–98.
35. Patel S, Berry L, Chan A. Covalent antithrombin-heparin complexes. *Thromb Res* **2007**; 120: 151–60.
36. Rabenstein DL. Heparin and heparan sulfate: structure and function. *Nat Prod Rep* **2002**; 19: 312–31.
37. Grootenbuis PDJ, Boeckel CAA Van. Constructing a Molecular Model of the Interaction between Antithrombin III and a Potent Heparin Analogue. *J Am Chem Soc* **1991**; 113: 2743–7.
38. Platé N a, Valuev LI. On the mechanism of enhanced thromboresistance of polymeric materials in the presence of heparin. *Biomaterials* **1983**; 4: 14–20.

39. Gott VL, Daggett RL. Serendipity and the development of heparin and carbon surfaces. *Ann Thorac Surg* **1999**; 68: S19–22.
40. Murugesan S, Xie J, Linhardt RJ. Immobilization of heparin: approaches and applications. *Curr Top Med Chem* **2008**; 8: 80–100.
41. Medtronic. CBAS, Carmeda BioActive Surface [Internet]. [cited 2013 Jan 16]. Available from: <http://www.carmeda.se/upl/files/31627.pdf>
42. Norbert Weber, Hans P. Wendel GZ. Hemocompatibility of heparin-coated surfaces and the role of selective plasma protein adsorption. *Biomaterials* **2002**; 23: 429–39.
43. Ovrum E, Tangen G, Tollofsrud S, Skeie B, Ringdal MAL, Istad R, Oystese R. Heparinized cardiopulmonary bypass circuits and low systemic anticoagulation: an analysis of nearly 6000 patients undergoing coronary artery bypass grafting. *J Thorac Cardiovasc Surg The American Association for Thoracic Surgery*; **2011**; 141: 1145–9.
44. Patel S, Berry L, Chan A. Analysis of inhibition rate enhancement by covalent linkage of antithrombin to heparin as a potential predictor of reaction mechanism. *J Biochem* **2007**; 141: 25–35.
45. Chan A, Paredes N, Thong B, Chindemi P, Paes B, Berry L, Monagle P. Binding of heparin to plasma proteins and endothelial surfaces is inhibited by covalent linkage to antithrombin. *Thromb Haemost* **2004**; 91: 1009–18.
46. Chan A, Berry L, Paredes N, Parmar N. Isoform composition of antithrombin in a covalent antithrombin–heparin complex. *Biochem Biophys Res Commun* **2003**; 309: 986–91.
47. Berry L, Andrew M, Chan A. Antithrombin-heparin complexes. In: Dumitriu S, editor. *Polymeric Biomaterials* New York, USA: Marcel Dekker Inc.; **2000**.
48. Sask KN, McClung WG, Berry L, Chan A, Brash JL. Immobilization of an antithrombin-heparin complex on gold: anticoagulant properties and platelet interactions. *Acta Biomater* **2011**; 7: 2029–34.
49. Wu W-I, Sask KN, Brash JL, Selvaganapathy PR. Polyurethane-based microfluidic devices for blood contacting applications. *Lab Chip* **2012**; 12: 960–70.
50. Klement P, Du YJ, Berry L, Andrew M, Chan A. Blood-compatible biomaterials by surface coating with a novel antithrombin-heparin covalent complex. *Biomaterials* **2002**; 23: 527–35.

51. Du YJ, Klement P, Berry L, Tressel P, Chan A. In vivo rabbit acute model tests of polyurethane catheters coated with a novel antithrombin-heparin covalent complex. *Thromb Haemost* **2005**; 94: 366–72.
52. Klement P, Du YJ, Berry L, Tressel P, Chan A. Chronic performance of polyurethane catheters covalently coated with ATH complex: a rabbit jugular vein model. *Biomaterials* **2006**; 27: 5107–17.
53. Bartzoka BV, Mcdermott MR, Brook MA. Protein \pm Silicone Interactions. *Adv Mater* **1999**; 11: 257–9.
54. Klenkler BJ, Chen H, Chen Y, Brook MA. A high-density PEG interfacial layer alters the response to an EGF tethered polydimethylsiloxane surface. *J Biomater Sci Polym Ed* **2008**; 19: 1411–24.
55. Chen H, Wang L, Zhang Y, Li D, McClung WG, Brook MA, Sheardown H, Brash JL. Fibrinolytic Polydimethyl siloxane) Surfaces. *Macromol Biosci* **2008**; 8: 863–70.
56. Olander B, Wirsén A, Albertsson A. Argon Microwave Plasma Treatment and Subsequent Hydrosilylation Grafting as a Way To Obtain Silicone Biomaterials with Well-Defined Surface Structures. *Biomacromolecules* **2002**; 3: 505–10.
57. Chen H, Brook MA, Chen Y, Sheardown H. Surface properties of PEO-silicone composites: reducing protein adsorption. *J Biomater Sci Polym Ed* **2005**; 16: 531–48.
58. Olander B, Wirsén A, Albertsson A-C. Silicone Elastomer Surface Functionalized with Primary Amines and Subsequently Coupled with Heparin. *Biomacromolecules* **2003**; 4: 145–8.
59. Achyuta AKH, Stephens KD, Lewis HGP, Murthy SK. Mitigation of Reactive Human Cell Adhesion on Poly (dimethylsiloxane) by Immobilized Trypsin. *Langmuir* **2010**; 26: 4160–7.
60. Amoako K a, Cook KE. Nitric oxide-generating silicone as a blood-contacting biomaterial. *ASAIO J* **2011**; 57: 539–44.
61. Zhang H, Annich GM, Miskulin J, Osterholzer K, Merz SI, Bartlett RH, Meyerhoff ME. Nitric oxide releasing silicone rubbers with improved blood compatibility: preparation, characterization, and in vivo evaluation. *Biomaterials* **2002**; 23: 1485–94.

62. Haemoscope Corporation. TEG 5000 User's Manual, Version 4 Software, Remote & TEG-enabled versions. **1999**.
63. Reikvam H, Steien E, Hauge B, Liseth K, Hagen KG, Storkson R, Hervig T. Thrombelastography. *Transfus Apher Sci* **2009**; 40: 119–23.
64. Peng HT. Thromboelastographic study of biomaterials. *J Biomed Mater Res B* **2010**; 94: 469–85.
65. Shankarraman V, Davis-Gorman G, Copeland JG, Caplan MR, McDonagh PF. Standardized methods to quantify thrombogenicity of blood-contacting materials via thromboelastography. *J Biomed Mater Res B* **2012**; 100: 230–8.
66. Klement P, Berry L, Liao P, Wood H, Tressel P, Smith LJ, Haque N, Weitz JI, Hirsh J, Paredes N, Chan A. Antithrombin-heparin covalent complex reduces microemboli during cardiopulmonary bypass in a pig model. *Blood* **2010**; 116: 5716–23.
67. Alibeik S, Zhu S, Yau JW, Weitz JI, Brash JL. Surface modification with polyethylene glycol-corn trypsin inhibitor conjugate to inhibit the contact factor pathway on blood-contacting surfaces. *Acta Biomater* **2011**; 7: 4177–86.
68. Atkinson HM, Mewhort-Buist TA, Berry L, Chan A. Anticoagulant mechanisms of covalent antithrombin-heparin investigated by thrombelastography. Comparison with unfractionated heparin and low-molecular-weight heparin. *Thromb Haemost* **2009**; 102: 626–8.
69. Chen H, Zhang Y, Li D, Hu X, Wang L, McClung WG, Brash JL. Surfaces having dual fibrinolytic and protein resistant properties by immobilization of lysine on polyurethane through a PEG spacer. *J Biomed Mater Res A* **2009**; 90: 940–6.
70. Sask KN, Berry L, Chan A, Brash JL. Modification of polyurethane surface with an antithrombin-heparin complex for blood contact: influence of molecular weight of polyethylene oxide used as a linker/spacer. *Langmuir* **2012**; 28: 2099–106.
71. Knight LC, Olexa S a, Malmud LS, Budzynski a Z. Specific uptake of radioiodinated fragment E1 by venous thrombi in pigs. *J Clin Invest* **1983**; 72: 2007–13.
72. Crowther M a, Berry LR, Monagle PT, Chan A. Mechanisms responsible for the failure of protamine to inactivate low-molecular-weight heparin. *Br J Haematol* **2002**; 116: 178–86.

73. Archambault J, Brash JL. Protein resistant polyurethane surfaces by chemical grafting of PEO: amino-terminated PEO as grafting reagent. *Colloids Surf B Biointerfaces* **2004**; 39: 9–16.
74. Berry L, Stafford A, Fredenburgh J, O’Brodivich H, Mitchell L, Weitz J, Andrew M, Chan A. Investigation of the anticoagulant mechanisms of a covalent antithrombin-heparin complex. *J Biol Chem* **1998**; 273: 34730–6.
75. Unsworth LD, Sheardown H, Brash JL. Polyethylene oxide surfaces of variable chain density by chemisorption of PEO-thiol on gold: adsorption of proteins from plasma studied by radiolabelling and immunoblotting. *Biomaterials* **2005**; 26: 5927–33.
76. Marois Y, Be MC. Studies of Primary Reference Materials Low-Density Polyethylene and Polydimethylsiloxane: A Review. *J Biomed Mater Res* **2001**; 58: 467–77.
77. Cornelius RM, Brash JL. Identification of proteins adsorbed to hemodialyser membranes from heparinized plasma. *J Biomater Sci Polym Ed* **1992**; 4: 291–304.
78. McDonnell E, Lyons G, Chau S. Effects of storing blood in citrated silicone-coated glass tubes vs. citrated plastic tubes on thromboelastograph variables. *Eur J Anaesthesiol* **2007**; 24: 291–2.
79. McNulty SE, Maguire DP, Thomas RE. Effect of heparin-bonded pulmonary artery catheters on the activated coagulation time. *J Cardiothorac Vasc Anesth* **1998**; 12: 533–5.
80. Wu W, Rochow N, Fusch G, Kusdaya R, Choi A, Selvaganapathy PR, Fusch C. Development of Microfluidic Oxygenators as Lung Assisting Devices for Preterm Infants. *15th International Conference on Miniaturized Systems for Chemistry and Life Sciences* Seattle, Washington, USA; **2011**. p. 550–2.
81. Rochow N, Wu W, Chan E, Nagpal D, Fusch, G Selvaganapathy, P Monkman S, Fusch C. Integrated microfluidic oxygenator bundles for blood gas exchange in premature infants. *IEEE 25th International Conference on Micro Electro Mechanical Systems (MEMS)* **2012**. p. 957 – 60.
82. Turbill P, Beugeling T, Poot AA. Proteins involved in the Vroman effect during exposure of human blood plasma to glass and polyethylene. *Biomaterials* **1996**; 17: 1279–87.

83. Kang SM, Hwang NS, Yoem J, Park SY, Messersmith PB, Choi I, Langer R, Anderson DG, Haeshin L. One-Step Multipurpose Surface Functionalization by Adhesive Catecholamine. *Adv Funct Mater* **2012**; 2949–55.
84. Lee Y Bin, Shin YM, Lee J-H, Jun I, Kang JK, Park J-C, Shin H. Polydopamine-mediated immobilization of multiple bioactive molecules for the development of functional vascular graft materials. *Biomaterials* **2012**; 33: 8343–52.
85. Thami T, Nasr G, Bestal H. Functionalization of Surface-Grafted Polymethylhydrosiloxane Thin Films with Alkyl Side Chains. *J Polym Sci A Polym Chem* **2008**; 46: 3546–62.
86. Guo D, Han H, Xiao S, Dai Z. Surface-hydrophilic and protein-resistant silicone elastomers prepared by hydrosilylation of vinyl poly(ethylene glycol) on hydrosilanes-poly (dimethylsiloxane) surfaces. *Colloids Surf A Physicochem Eng Asp* **2007**; 308: 129–35.
87. Li WH, Zhang XY, Dai JB. Synthesis and characterization of a novel hydroxypolyether blocked polydimethylsiloxane PEO-b-PDMS-b-PEO. *Chin Chem Lett* **2008**; 19: 1209–11.
88. Tsai C, Chang Y, Sung H, Hsu J, Chen C. Effects of heparin immobilization on the surface characteristics of a biological tissue fixed with a naturally occurring crosslinking agent (genipin): an in vitro study. *Biomaterials* **2001**; 22: 523–33.
89. Chen H, Brook MA, Sheardown H, Chen Y, Klenkler BJ. Generic Bioaffinity Silicone Surfaces. *Bioconjug Chem* **2006**; 17: 21–8.
90. Sefton M V, Gemmell CH, Gorbet MB. What really is blood compatibility?*. *J Biomater Sci Polym Ed* **2000**; 11: 1165–82.